Geobios 86 (2024) 49–64

Contents lists available at ScienceDirect

Geobios

journal homepage: www.elsevier.com/locate/geobio

Research Paper

New Insights on the Upper Triassic Silves Group in Algarve Basin, Portugal: Palynological, paleophytogeography and paleoclimatology advances ☆

Margarida Vilas-Boas [a,*], Zélia Pereira [b], Simonetta Cirilli [c], Paulo Fernandes [a]

[a] CIMA, Centre of Marine and Environmental Research|ARNET - Infrastructure Network in Aquatic Research, University of Algarve, Campus de Gambelas, 8000-139 Faro, Portugal
[b] LNEG, Laboratório Nacional de Energia e Geologia, Rua da Amieira, 4465-965 S. Mamede de Infesta, Porto, Portugal
[c] Dipartimento di Fisica e Geologia, Università degli Studi di Perugia, 06123 Perugia, Italy

ARTICLE INFO

Article history:
Received 26 September 2023
Accepted 5 August 2024
Available online 19 September 2024

Keywords:
Sporomorphs
Palynostratigraphy
Paleophytogeography
Carnian
Rhaetian
Triassic/Jurassic Boundary

ABSTRACT

This paper presents the results of palynostratigraphic studies in the Silves Group in the Algarve Basin, Portugal. From bottom to top comprises the Silves Sandstones, the Silves Marl-Carbonate Evaporitic Complex, and the Volcano-Sedimentary Series. This study aims to detail the age of the Silves Group, bracketing the Triassic-Jurassic transition, using palynology. For this purpose, 250 samples were collected from 14 main sections. Previous results from a section above the Variscan unconformity, enabled to date the base of the Silves Sandstones and the onset of the Mesozoic sedimentary cycle in the Algarve Basin to lower Carnian. In this work, the top of the Silves Sandstones, containing *Camerosporites secatus*, *Enzonalasporites vigens*, *Granuloperculatipollis rudis*, *Lagenella martinii*, *Patinasporites densus*, *Samaropollenites speciosus*, and *Vallasporites ignacii*, is dated to the upper Carnian. The base of the Silves Marl-Carbonate Evaporitic Complex, consisting of *Alisporites* sp., *Araucariacites australis*, *Classopollis meyerianus*, *Classopollis torosus*, *Paracirculina quadruplicis* and *Triadispora* sp., indicates an upper Carnian age. The presence of *Alisporites diaphanus*, *Araucariacites australis*, *Cerebropollenites macroverrucosus, Classopollis meyerianus*, *Classopollis torosus*, *Perinopollenites elatoides*, *Calamospora mesozoica*, and *Kraeuselisporites reissingeri* allows to date the top of the Silves Marl-Carbonate Evaporitic Complex as upper Rhaetian-lower Hettangian. This study allows to date the Silves Group in the Algarve Basin from the lower Carnian to lower Hettangian (Triassic-Jurassic boundary) for the first time. The Carnian microflora provides new insights of the Onslow Microflora in the Western Tethys.

1. Introduction and geological setting

The Algarve Basin (AB), located in the South of Portugal (Fig. 1 (A)), is a Mesozoic sedimentary basin that formed during the breakup of Pangaea and subsequent extensional tectonic events that led to the opening of the North Atlantic Ocean (Terrinha et al., 2013). The initial sedimentary infill of the AB consists of continental siliciclastic red beds, volcanics, and evaporites, collectively known as the Silves Group. It unconformably overlies Carboniferous turbidites, which were deformed and underwent low-grade metamorphism during the Variscan Orogeny (Palain, 1976; Terrinha et al., 2013).

The Silves Group comprises sedimentary rocks deposited in various environments, ranging from continental, primarily alluvial, to shallow marine evaporitic settings (Terrinha et al., 2006). The group comprises three stratigraphic units, arranged from base to top: the Silves Sandstones, the Silves Marl-Carbonate Evaporitic Complex, and the Volcano-Sedimentary Series.

The sedimentary facies, textures, and thickness of the Silves Sandstones vary depending on their position within the AB. In outcrops west of the São Marcos da Serra-Quarteira Fault (SMSQF; Fig. 1(B)), the Silves Sandstone succession begins at the base with 6 to 10 m thick mudstones and siltstones (São Bartolomeu de Messines Clays; Palain, 1976). Above the last beds are coarse to fine-grained reddish sandstones displaying cross-stratification and lamination and trough cross-stratification, without any interbedded clay and silt size sediment (Fig. 2). Massive strata usually display an erosive basal surface followed by gravel lags as channel-fill deposits. The facies and sedimentary structures suggest deposition in fluvial settings. The absence of significant

☆ Corresponding editor: Evelyn Kustatscher.
* Corresponding author.
E-mail address: amvilasboas@ualg.pt (M. Vilas-Boas).

https://doi.org/10.1016/j.geobios.2024.08.001
0016-6995/

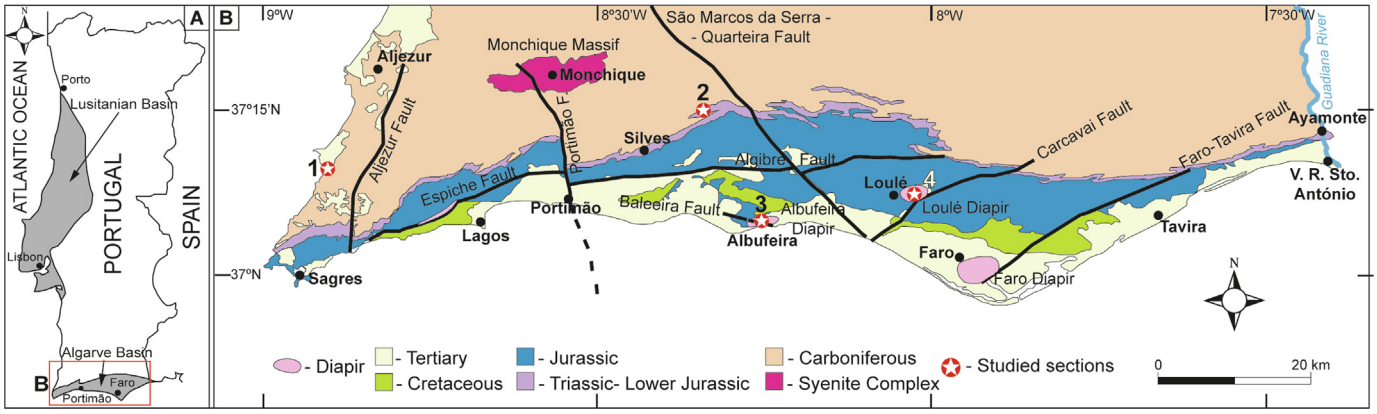

Fig. 1. Map of the studied area with location of studied sections. **A.** Map of Portugal with the Lusitanian and Algarve basins represented. The red rectangle represents the area of the studied sections. **B.** Detailed geological map of the Algarve Basin with the studied sections signed by the star symbol. 1: Amado Beach section; 2: Amorosa section; 3: Albufeira Diapir section; 4: Loulé Rock Salt Mine; SMSQF: São Marcos da Serra-Quarteira Fault; AF: Algibre Fault. (For interpretation of the references to color in this figure legend, the reader is referred to the web version of this article.)

floodplain deposits suggests deposition by bedload-dominated (braided) river systems. East of the SMSQF, the Silves Sandstones unit shows most of the aforementioned features except for the absence of mudstones at the base, coarser clastic sediments, and matrix-supported conglomerates interbedded with the sandstones (Fig. 2). These differences suggest a more pronounced tectonic control on sedimentation in the eastern part of the SMSQF and a shorter distance to the sediment source regions.

The Silves Marl-Carbonate Evaporitic Complex conformably overlies the Silves Sandstones unit. Similar to the Silves Sandstones, the stratigraphy of this unit is strongly influenced by tectonic controls showing a lack in evaporitic deposits are absent to the north of the west-east trending Algibre Fault (AF; Fig. 1(B)). South of this fault, evaporites are only found in diapirs that intrude into Jurassic and Lower Cretaceous sedimentary rocks, such as the Loulé and Albufeira diapirs.

North of the AF, the Silves Marl-Carbonate Evaporitic Complex consists of variegated mudstones interbedded with marls, fine-grained sandstones, and siltstones reaching a maximum thickness of over 100 m. Sedimentary structures observed in this unit include rare wave ripples, current ripples, parallel laminations, desiccation cracks, bioturbations, and pedogenic structures. Fossils found within this unit, including bivalves (*Eustheria* sp.; Palain, 1976) and vertebrate remains of *Phytosauria* (Mateus et al., 2014) and *Metoposaurus* (Brusatte et al., 2015), indicate an Upper Triassic age for this unit. In the town of Ayamonte, located near the Portuguese-Spanish border, the upper part of this unit is carbonate-rich. It has yielded a relatively rich fauna of bivalves, ostracods, gastropods (Santos et al., 2022), and a rare neural arch of a sauropterygian reptile (Reolid et al., 2022). These recent palaeontological data further support an Upper Triassic age for this portion of the Silves Marl-Carbonate Evaporitic Complex. The sedimentary structures and the fossils from this stratigraphic unit suggest deposition in a shallow lacustrine environment frequently affected by desiccation events (ephemeral lakes).

The stratigraphic sequence of the Silves Group is topped by the Volcano-Sedimentary Series, which primarily comprises pyroclasts and a few basalt flows, indicating a prevalence of explosive volcanism over effusive phases. The basalt flow located at the uppermost part of this unit was dated using radio-isotopic analysis based on $^{40}Ar/^{39}Ar$, and it was assigned an age of 198.1 ± 0.4 Ma (Lower Jurassic). This age was correlated with the Central Atlantic Magmatic Province (CAMP) showing consistency with a palynological assemblage discovered in mudstones approximately 50 m below the dated basalt flow (Verati et al., 2007).

The present research aims to refine the ages and to obtain palaeoenvironmental information, such as new insights into the of the Onslow Microflora, of the Upper Triassic-Lower Jurassic stratigraphic record of the Silves Group in the Algarve Basin through palynology. To achieve this goal, 250 samples were collected from 14 stratigraphic sections, which were subsequently analysed to establish a detailed palynostratigraphic age based on the identification of key palynomorph taxa.

2. Material and methods

2.1. Studied sections

2.1.1. Amorosa section

This section is a roadcut outcrop located south of the village of Amorosa (37°15'38.65"N; 8°19'11.66"W) and exposes the stratigraphic limit between the Silves Sandstone and the Silves Marl-Carbonate Evaporitic Complex (Figs. 1, 2). The section is ca. 6 m thick, composed at the base of reddish silty mudstones that pass upward abruptly to a 1.2 m-thick red sandstone bed (Fig. 3(A)). The sandstone bed shows an erosive base, normal grading, cross-bedding and cross-lamination. Overlying the sandstone bed is a ca. 2 m thick of reddish silty mudstones with pedogenic structures, which pass gradually upwards to grey mudstones having thin beds of micrite limestone interbedded (Fig. 3(A)). The sample with palynological results (AMOROSA 4(−20 cm); Fig. 2) corresponds to the basal layers of the Silves Marl-Carbonate Evaporitic Complex.

2.1.2. Amado Beach section

This section is exposed along the northern seacliffs at Amado Beach near the Carrapateira village (37°10'9.37"N; 8°54'10.72"W; Figs. 1, 2). The section is ca. 61 m thick and depicts the upper part of the Silves Sandstones and the lower part of the Silves Marl-Carbonate Evaporitic Complex.

The Silves Sandstones are a ca. 17 m thick sequence showing cross-bedding, trough cross-bedding, cross-lamination, normal grading, and basal erosional surfaces, often having matrix-supported conglomerates above. No mudstones or siltstone beds are interbedded with the sandstones, indicating that this sequence relates to amalgamated beds, probably due to the aggradation of channel fill deposits.

A 0.7 m-thick bed consisting of fine-grained sandstones and siltstones showing current ripples and cross-laminations, sometimes showing climbing laminae separates the Silves Sandstones

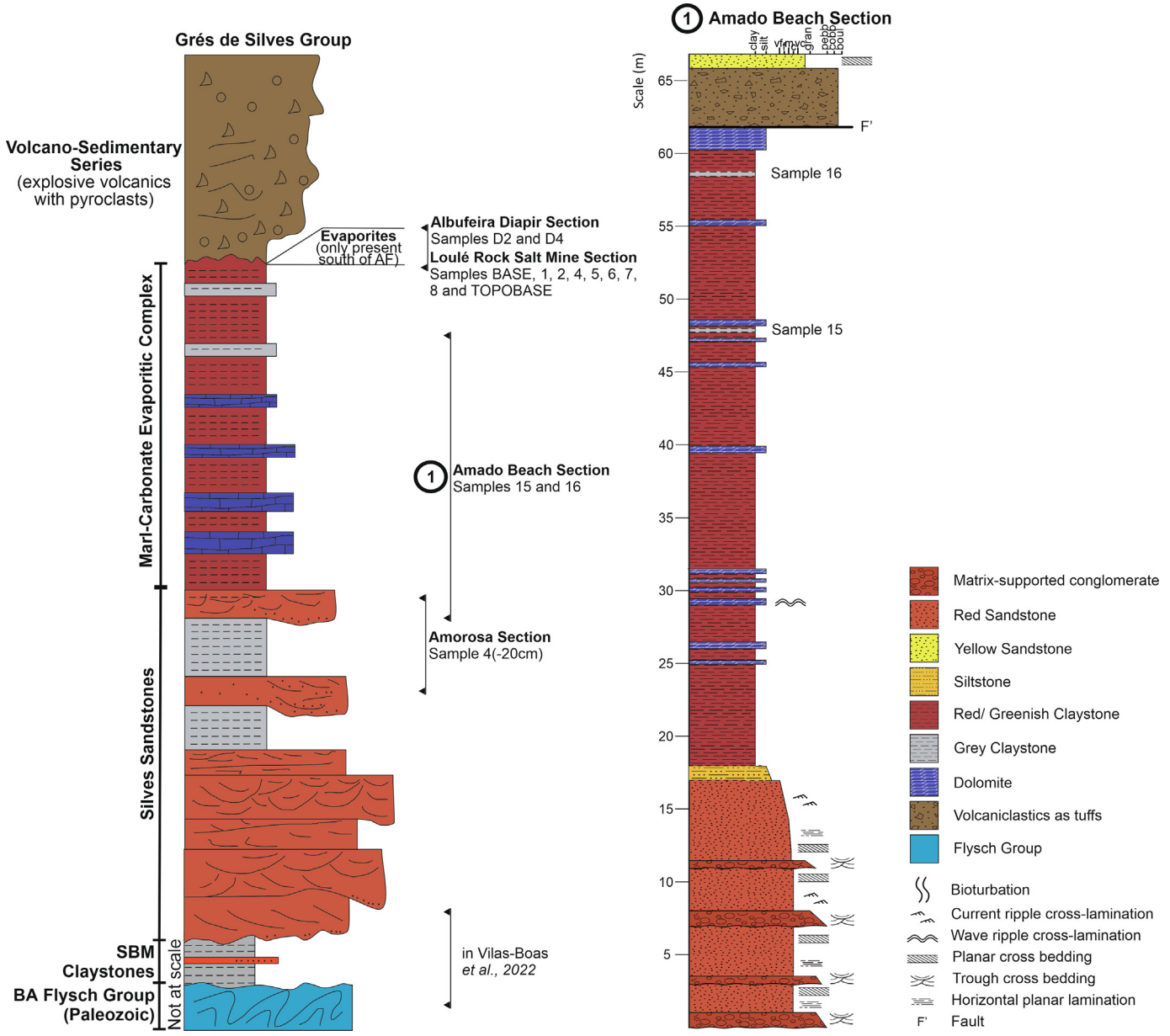

Fig. 2. General stratigraphic log of the Silves Group with location of the studied sections and productive samples. 1: Detailed log of Amado Beach section with the productive samples signed. AF: Algibre Fault; SBM Claystones: São Bartolomeu de Messines Clays; BA Flysch Group: Baixo-Alentejo Flysch Group. (For interpretation of the references to color in this figure legend, the reader is referred to the web version of this article.)

from the ca. 45 m thick mudstone dominant sequence belonging to the Silves Marl-Carbonate Evaporitic Complex (Figs. 2, 3(B)). The mudstones are variegated (reddish to grey). They are interbedded with thin dolomite beds and fine-grained sandstones, occasionally showing wave ripples with reduction spots and whirls (Figs. 2, 3 (B)). The grey-to-dark mudstones and the dolomite beds often show parallel laminations. This part of the Amado Beach sequence is intruded by dolerites and is in contact with volcanic rocks (mafic tuffs) of the Volcano-Sedimentary Series through a fault. Two samples yielded palynological results located in the uppermost part of the Marl-Carbonate Evaporitic Complex.

2.1.3. Loulé Rock Salt Mine section

The underground gallery (N01G01N between N01C0100 and N01C0101, located at 230 m deep) of the Loulé Rock Salt Mine (37°8'5.53"N; 8°0'28.05"W; Figs. 1, 2) intersects a ca. 1 m thick mudstone bed intercalated with the massive halite beds (Fig. 3 (C)). The mudstone bed is structureless and shows grey to dark-grey colour. Eight samples were taken from the mudstone bed, and two additional samples were collected from the impure halite at the bottom and top of the mudstone bed.

2.1.4. Albufeira Diapir section

The Albufeira's Diapir is exposed at the seacliff of Baleeira's Cove, west of the town of Albufeira (37°4'54.18"N; 8°15'45.27" W; Figs. 1, 2). This diapir is fault-controlled by the East-West trending Baleeira Fault, and the bedding is difficult to recognize within the diapir outcrop. The evaporite consists mainly of anhydrite and gypsum intercalated with very thin lenses of grey mudstone (Fig. 3(D)). Two samples were taken from the grey mudstones.

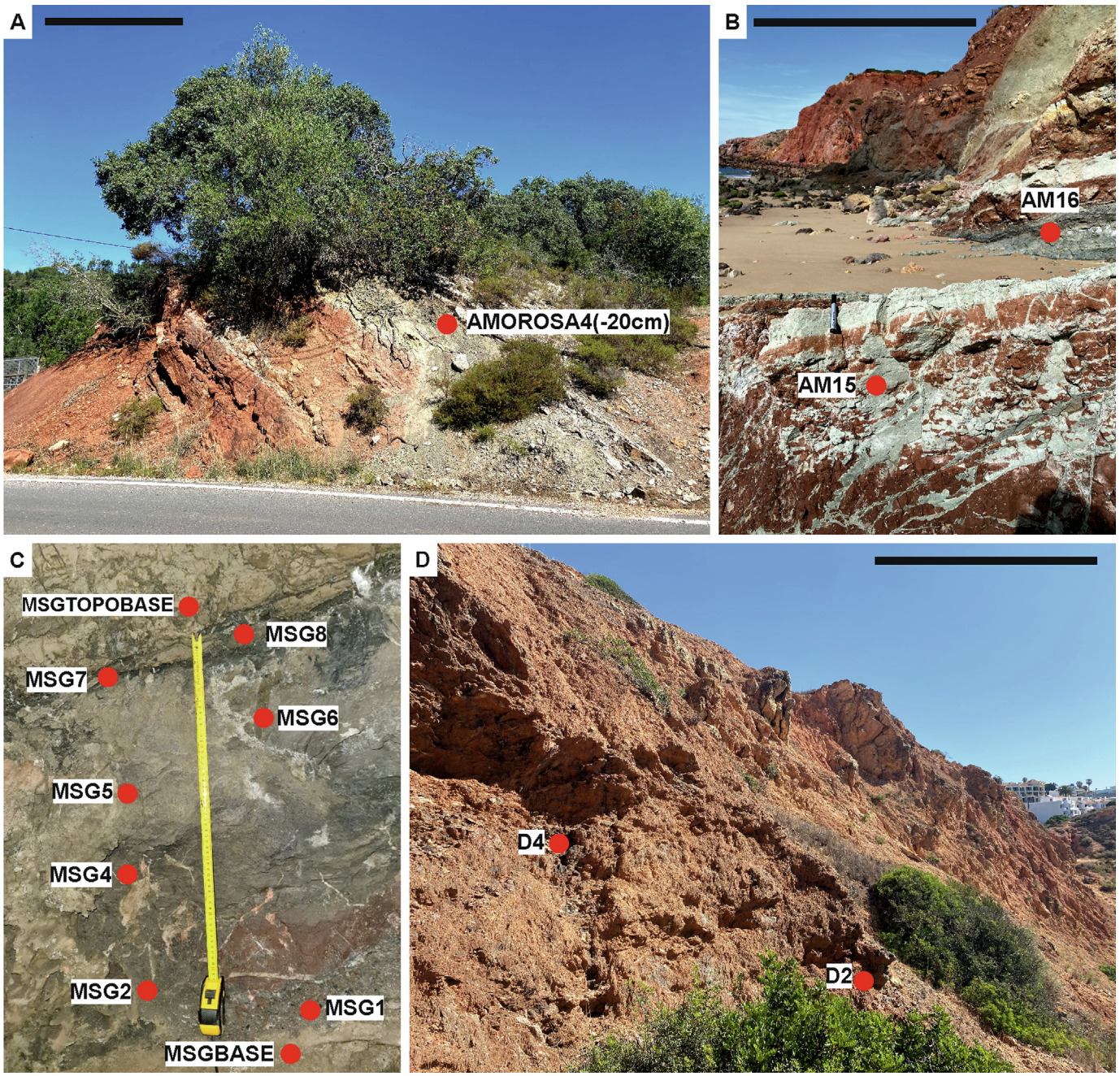

Fig. 3. Field photographies of the studied sections, with location of the productive samples signed by the red dot. **A.** Amorosa section. **B.** Amado Beach section. **C.** Loulé Rock Salt Mine section (measuring tape marks 0.61 m). **D.** Albufeira Diapir section. Scale bars: 1 m (A, B, D). (For interpretation of the references to color in this figure legend, the reader is referred to the web version of this article.)

2.2. Palynology

Forty-three samples were collected from four sections that yielded productive samples for palynological studies in the Silves Group of the Algarve Basin. Twenty-nine samples were collected from the Silves Sandstones unit along the Amorosa and Amado Beach sections, while fourteen samples were collected from the Silves Marl-Carbonate Evaporitic Complex along the Loulé Rock Salt Mine and Albufeira's Diapir sections. Fourteen of the forty-three samples were productive, showing moderate to well-preserved sporomorphs. In the Amorosa area, three sections were sampled along the M1080 road in the Vale Fuzeiros, close to São Bartolomeu de Messines. Ten samples were collected from these three sections, with one of them being positive: AMOROSA 4(−20 cm). From Amado Beach, located south of Aljezur, nineteen samples were collected (positive samples: AM15 and AM16). Ten samples were collected in the Loulé Rock Salt Mine (positive samples: MSGBASE, MSG 1, MSG2, MSG4, MSG5, MSG6, MSG7, MSG8 and MSGTOPOBASE). Four samples were collected from the Diapir in Baleeira Cove, Albufeira (positive samples: D2 and D4).

Standard palynological laboratory techniques were employed for organic matter extraction and concentration, including treatments with hydrochloric (HCl) and hydrofluoric (HF) acids (Wood et al., 1996; Riding and Warny, 2008). The residues were sieved through a 15 µm sieve and mounted on microscope slides using Entelan®, a commercially available resin-based mounting

Table 1
Dataset for terrestrial palynomorphs (spores and pollen grains, in %) and marine palynomorphs (algae). X: Registered outside the count.

Silves Group Units	**Silves Sandstones**			**Silves Marl-Carbonate Evaporitic Complex**											
Age of the Section	**Upper Triassic - upper Carnian**			**Upper Triassic - Rhaetian**						**Lower Jurassic - Hettangian**				**? Rhaetian- ? Hettangian**	
Sections	**Amorosa**	**Amado's Beach**		**Loulé Rock Salt Mine**										**Albufeira's Diapir**	
Samples	**4(-20 cm)**	**15**	**16**	**BASE**	**1**	**2**	**3**	**4**	**5**	**6**	**7**	**8**	**TOPO BASE**	**D2**	**D4**
POLLEN															
Alisporites diaphanus											X				
Alisporites sp.		3.8	3		0.4										
Araucariacites australis				X						X		X			
Araucariacites sp.				17.5	24.9			10.2	14.3	36.7	18.7	48	36.1	6.4	31.2
Camerosporites secatus		X													
Cerebropollenites macroverrucosus										0.4					
Cerebropollenites sp.										0.4	0.4	0.4			
Classopollis malformed										X	X			21.6	6.8
Classopollis meyerianus				61.4	67.5			44.9	64.3	26.7	46	31.6	41	22.4	13.2
Classopollis sp.				7	0.4	0.6		18.4		2.4	0.4			8	1.2
Classopollis torosus										29.9	31.5	17.2	22.3	32.4	24.8
Cycadopites sp.				5.3						0.8	0.4	0.8			
Ellipsovelatisporites sp.	2.5		0.4												
Enzonalasporites vigens		X	9												
Ephedripites sp.												X			
Granuloperculatipollis rudis			0.4												
Lagenella martinii			X												
Microcachrydites doubingeri			2.2												
Microcachrydites fastidioides			1.9												
Microcachrydites sp.		3.4	1.5												
Paracirculina malformed	17.3														
Paracirculina quadruplicis	50.6	8.3	25.5	3.5											
Paracirculina sp.	4.9	0.4	4.9												
Patinasporites densus	X	0.7	7.5												
Perinopollenites elatoides										2.4	2.6				
Samaropollenites speciosus	2.5	2.6	38.9												
Triadispora sp.	12.3	X	1.9					2							
Vallasporites ignacii	1.2	X	0.4												
Sum Pollen	91.3	19.2	97.5	94.7	93.2	0.6	0	75.5	78.6	99.7	100	98	99.4	90.8	77.2
SPORES															
Anapiculatisporites sp.											X				
Calamospora mesozoica					X					X					
Calamospora sp.		X										0.4			
Carnisporites sp.														6	1.2
Convolutispora sp.	0.6	X													
Deltoidospora sp.											X			0.4	
Deltoidospora toralis											X				
Kraeuselisporites reissingeri	0.6											1.6	0.6		
Kraeuselisporites sp.												X			
Kyrtomisporis sp.										0.4					
Leptolepidites argentaeformis											X				
Playfordiaspora sp.	7.4	0.8	2.6		0.4										
Verrucosisporites sp.	X	X													
Sum Spores	8.6	0.8	2.6	0	0.4	0	0	0	0	0.4	0	2	0.6	6.4	1.2

(*continued on next page*)

Table 1 (*continued*)

Silves Group Units	Silves Sandstones			Silves Marl-Carbonate Evaporitic Complex											
Age of the Section	**Upper Triassic - upper Carnian**			**Upper Triassic - Rhaetian**					**Lower Jurassic - Hettangian**					**? Rhaetian- ? Hettangian**	
Sections	**Amorosa**	**Amado's Beach**		**Loulé Rock Salt Mine**										**Albufeira's Diapir**	
Samples	**4(-20 cm)**	**15**	**16**	**BASE**	**1**	**2**	**3**	**4**	**5**	**6**	**7**	**8**	**TOPO BASE**	**D2**	**D4**
ALGAE															
Algae sp. A		6.4													
Botryococcus sp.		0.8													
Leiosphaeridia sp.		52.1										X		2.8	21.6
Ovoidites sp.		X													
Plaesiodictyon mosellanum ssp. *bullatum*		7.5													
Plaesiodictyon mosellanum ssp. *variable*		12.1													
Plaesiodictyon sp.		1.1													
Reworked algae				5.3	6.4	99.4		24.5	21.4					2.8	21.6
Sum Algae		80	0	5.3	6.4	99.4	0	24.5	21.4	0	0	0	0		
TOTAL SUM	100	100	100	100	100	100	0	100	100	100	100	100	100	100	100

medium. The slides were examined using a Leica DM750 microscope equipped with a Leica ICC50W camera and a BX40 Olympus equipped with an Olympus CS50 digital camera. Semi-quantitative abundance was determined by counting, when possible, 250 specimens per slide. Additionally, three slides from each sample were examined for rare taxa outside the count, represented with an X in Table 1. Figs. 4–6 provide illustrations of the biostratigraphically significant taxa and a species list is given in Appendix A. All samples, residues, and slides are stored at the University of Algarve and the Palynological Collection of LNEG, Portugal.

3. Results

The sporomorph assemblages recorded in the studied successions are described and documented in Fig. 7. The quantitative and qualitative distribution of sporomorph associations is presented based on the relative abundance of prominent taxa, as well as the first appearance (FA), last appearance (LA), first appearance datum (FAD), last appearance datum (LAD), first occurrence (FO) and last occurrence (LO) of selected stratigraphically important taxa (Fig. 7; Table 1).

This study recognized three palynoassemblages (in stratigraphic order from oldest to youngest):

- **Palynoassemblage 1**. The microflora found in this assemblage is derived from the Amorosa and Amado Beach sections of the Silves Sandstones and the Silves Marl-Carbonate Evaporitic Complex units, respectively. It consists of twelve genera and ten species of moderate to well-preserved taxa of pollen, five genera and one species of spores, and four genera and two species of algae. The distinguishing feature of this assemblage is the concurrent presence of *Patinasporites densus*, *Samaropollenites speciosus*, *Vallasporites ignacii*, *Enzonalasporites vigens and Granuloperculatipollis rudis*, these last two taxa occurring for the first time in the Amado Beach section. Other consistently present taxa include *Paracirculina* sp., *Paracirculina quadruplicis*, *Playfordiaspora* sp., and *Triadispora* sp. Additionally, the assemblage includes *Alisporites* sp., *Camerosporites secatus*, *Ellipsovelatisporites* sp., *Lagenella martinii*, *Microcachrydites doubingeri*, *Microcachrydites fastidioides*, *Microcachrydites* sp., malformed specimens of *Paracirculina* sp., and spores such as *Calamospora* sp., *Convolutispora* sp., *Kraeuselisporites reissingeri*, and *Verrucosisporites* sp. The algal association consists of *Botryococcus* sp., *Leiosphaeridia* sp., *Ovoidites* sp., *Plaesiodictyon mosellanum* ssp. *bullatum*, *Plaesiodictyon mosellanum* ssp. *variable*, *Plaesiodictyon* sp., and of an undetermined species identified as Algae sp. A;
- **Palynoassemblage 2**. The samples containing this assemblage derive from the lower part of the Loulé Rock Salt Mine section that belongs to the Silves Marl-Carbonate Evaporitic Complex. The assemblage comprises moderate to well-preserved palynomorphs including six genera and three pollen species, two genera and one species of spores, and one species of algae. The notable feature of this assemblage is the FA of *Classopollis meyerianus*, *Classopollis torosus*, and *Classopollis* sp. Other components include the pollen *Alisporites* sp., *Araucariacites australis*, *Araucariacites* sp., *Cycadopites* sp., *Paracirculina quadruplicis* and *Triadispora* sp., and the spores *Calamospora mesozoica* and *Playfordiaspora* sp. Additionally, the palynoassemblage contains some specimens with fungal or algal affinity which appear to be reworked due to their darker color and resemblance to Neo-Proterozoic-age algae (e.g., *Ourasphaira giraldae*);
- **Palynoassemblage 3**. This assemblage derives from the upper part of the Loulé Rock Salt Mine section included in the Silves Marl-Carbonate Evaporitic Complex. It encompasses seven gen-

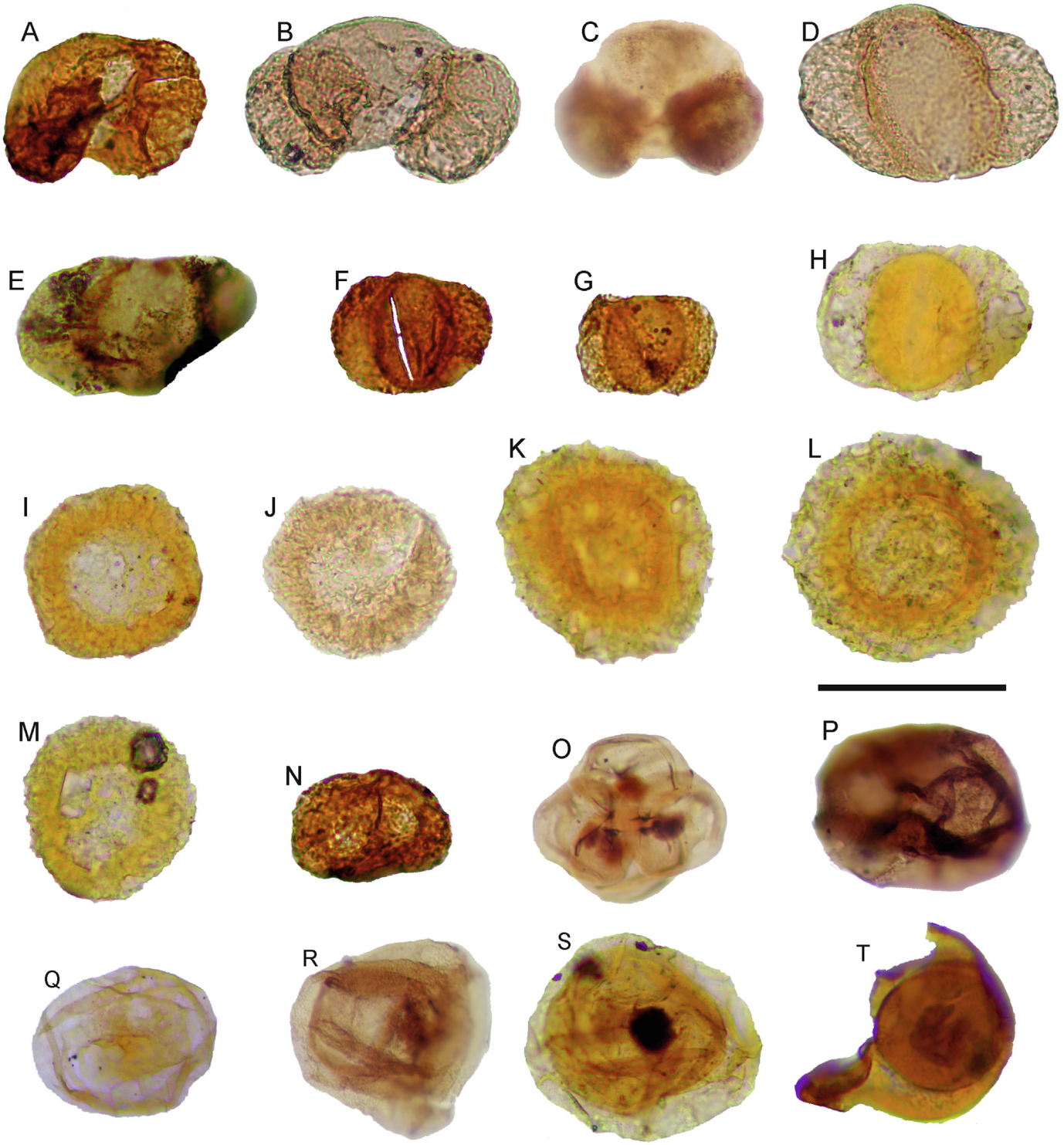

Fig. 4. Selected pollen grains from the Silves Group sections studied in this work. Species name is followed by the outcrop, sample, slide number and England Finder coordinates. **A.** *Samaropollenites speciosus* Goubin, 1965, outcrop Amorosa, sample Amorosa4(−20 cm), slide 1, EF J42|3. **B.** *Samaropollenites speciosus* Goubin, 1965, outcrop Amado's Beach, sample AM15, slide 1, EF Y40|3. **C.** *Microcachrydites* sp., outcrop Amado's Beach, sample AM15, slide 1, EF K33|1. **D.** *Alisporites* sp., outcrop Amado's Beach, sample AM15, slide 1, EF R29. **E.** *Alisporites diaphanus* (Pautsch, 1958) Lund, 1977, outcrop Rock Salt Mine, sample MSGvd7, slide 1, EF M29|2. **F.** *Triadispora* sp., outcrop Amorosa, sample Amorosa4(−20 cm), slide 1, EF R28. **G.** *Triadispora* sp., outcrop Amorosa, sample Amorosa4(−20 cm), slide 1, EF O23|3. **H.** *Triadispora* sp., outcrop Amado's Beach, sample AM16, slide 1Z, EF L42. **I.** *Enzonalasporites vigens* Leschik, 1956 emend. Scheuring, 1970, outcrop Amado's Beach, sample AM15, slide 1Z, EF O16. **J.** *Patinasporites densus* Leschik emend. Scheuring, 1970, outcrop Amado's Beach, sample AM15, slide 2, EF W35. **K.** *Patinasporites densus* Leschik emend. Scheuring, 1970, outcrop Amado's Beach, sample AM16, slide 1Z, EF J46. **L.** *Patinasporites densus* Leschik emend. Scheuring, 1970, outcrop Amado's Beach, sample AM16, slide 1Z, EF K41|2. **M.** *Vallasporites ignacii* Leschik, 1956 emend. Scheuring, 1970, outcrop Amado's Beach, sample AM16, slide 1Z, EF P43|3. **N.** *Vallasporites ignacii* Leschik, 1956 emend. Scheuring, 1970, outcrop Amorosa, sample Amorosa4(−20 cm), slide 1, EF S30. **O.** *Paracirculina quadruplicis* Scheuring, 1970, outcrop Amado's Beach, sample AM15, slide 1, EF N25. **P.** *Araucariacites australis* Cookson, 1947, outcrop Rock Salt Mine, sample MSGvdBASE, slide 1, EF O12|2. **Q.** *Araucariacites* sp., outcrop Amado's Beach, sample AM15, slide 1, EF L15. **R.** *Perinopollenites elatoides* Couper, 1958, outcrop Rock Salt Mine, sample MSGvd6, slide 1F, EF D40. **S.** *Perinopollenites elatoides* Couper, 1958, outcrop Rock Salt Mine, sample MSGvd7, slide 1F, EF R35. **T.** *Perinopollenites elatoides* Couper, 1958, outcrop Rock Salt Mine, sample MSGvd6, slide 1F, EF M38|3. Scale bar: 50 μm. (For interpretation of the references to color in this figure legend, the reader is referred to the web version of this article.)

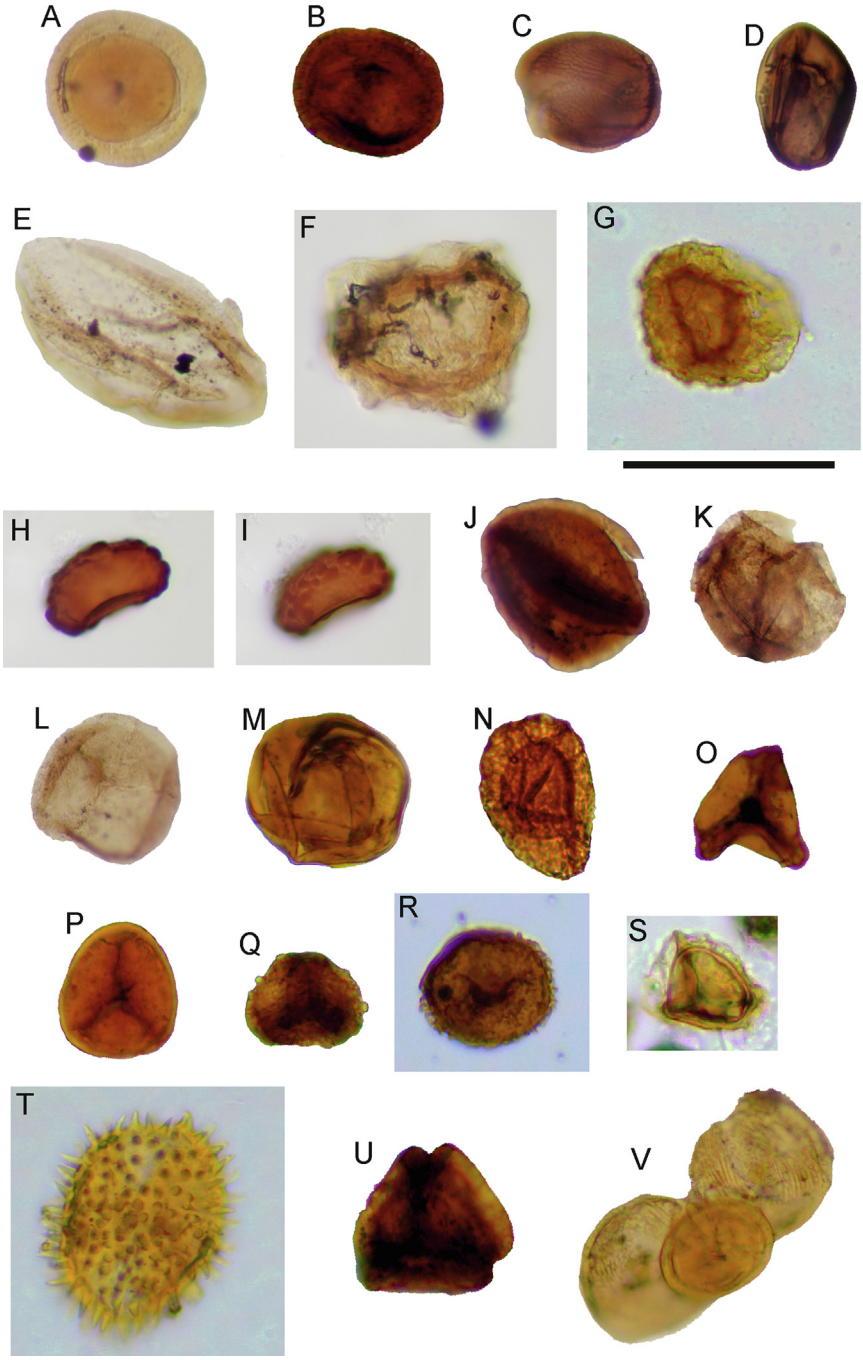

Fig. 5. Selected pollen grains (A-J) and spores (K-V) from the Silves Group sections studied in this work. Species name is followed by the outcrop, sample, slide number and England Finder coordinates. **A.** *Classopollis meyerianus* (Klaus) de Jersey, 1973, outcrop Rock Salt Mine, sample MSGvd8, slide 1F, EF T12|3. **B.** *Classopollis* sp., outcrop Rock Salt Mine, sample MSGvd6, slide 1, EF G34|1. **C.** *Classopollis torosus* Reissinger, 1950, outcrop Rock Salt Mine, sample MSGvd6, slide 1F, EF S34|4. **D.** *Cycadopites* sp., outcrop Rock Salt Mine, sample MSGvdBASE, slide 1, EF E41. **E.** *Ephedripites* sp., outcrop Rock Salt Mine, sample MSGvd8, slide 1F, EF N37|2. **F.** *Cerebropollenites* sp., outcrop Rock Salt Mine, sample MSGvd8, slide 1F, EF O29|1. **G.** *Cerebropollenites* sp., outcrop Rock Salt Mine, sample MSGvd7, slide 1F, EF C37|2. **H.** *Cerebropollenites* sp., outcrop Rock Salt Mine, sample MSGvd6, slide 1F, EF S28. **I.** *Cerebropollenites* sp., outcrop Rock Salt Mine, sample MSGvd6, slide 1F, EF S28. **J.** *Cerebropollenites macroverrucosus* (Thiergart) Schulz, 1967, outcrop Rock Salt Mine, sample MSGvd6, slide 1F, EF O20|3. **K.** *Calamospora mesozoica* Couper, 1958, outcrop Rock Salt Mine, sample MSGvd1, slide 1, EF V35|1. **L.** *Calamospora mesozoica* Couper, 1958, outcrop Rock Salt Mine, sample MSGvd5, slide 1F, EF L19. **M.** *Calamospora tener* (Leschik, 1955) Mädler, 1964, outcrop Rock Salt Mine, sample MSGvd7, slide 1F, EF R23|3. **N.** *Playfordiaspora* sp., outcrop Amorosa, sample Amorosa4(−20 cm), slide 1, EF F30. **O.** *Deltoidospora toralis* (Leschick) Lund, 1977, outcrop Rock Salt Mine, sample MSGvd7, slide 1F, EF T42. **P.** *Deltoidospora* sp., outcrop Rock Salt Mine, sample MSGvd7, slide 1F, EF Z39|1. **Q.** *Leptolepidites argaenteaeformis* (Bolkhovitina) Morbey, 1975, outcrop Rock Salt Mine, sample MSGvd7, slide 1F, EF M27|2. **R.** *Anapiculatisporites* sp., outcrop Rock Salt Mine, sample MSGvd7, slide 1F, EF N25. **S.** *Kraeuselisporites* sp., outcrop Rock Salt Mine, sample MSGvd8, slide 1, EF S31. **T.** *Carnisporites spiniger* (Leschik) Morbey, 1975, outcrop Albufeira's Diapir, sample D2, slide 3, EF M33. **U.** *Kyrtomisporis* sp., outcrop Rock Salt Mine, sample MSGvd6, slide 1F, EF M21|3. **V.** *Classopollis torosus* Reissinger, 1950, to outcrop Albufeira's Diapir, sample D2, slide 1, EF P21, tetrad with one abnormal *Classopollis* pollen. Scale bar: 50 μm. (For interpretation of the references to color in this figure legend, the reader is referred to the web version of this article.)

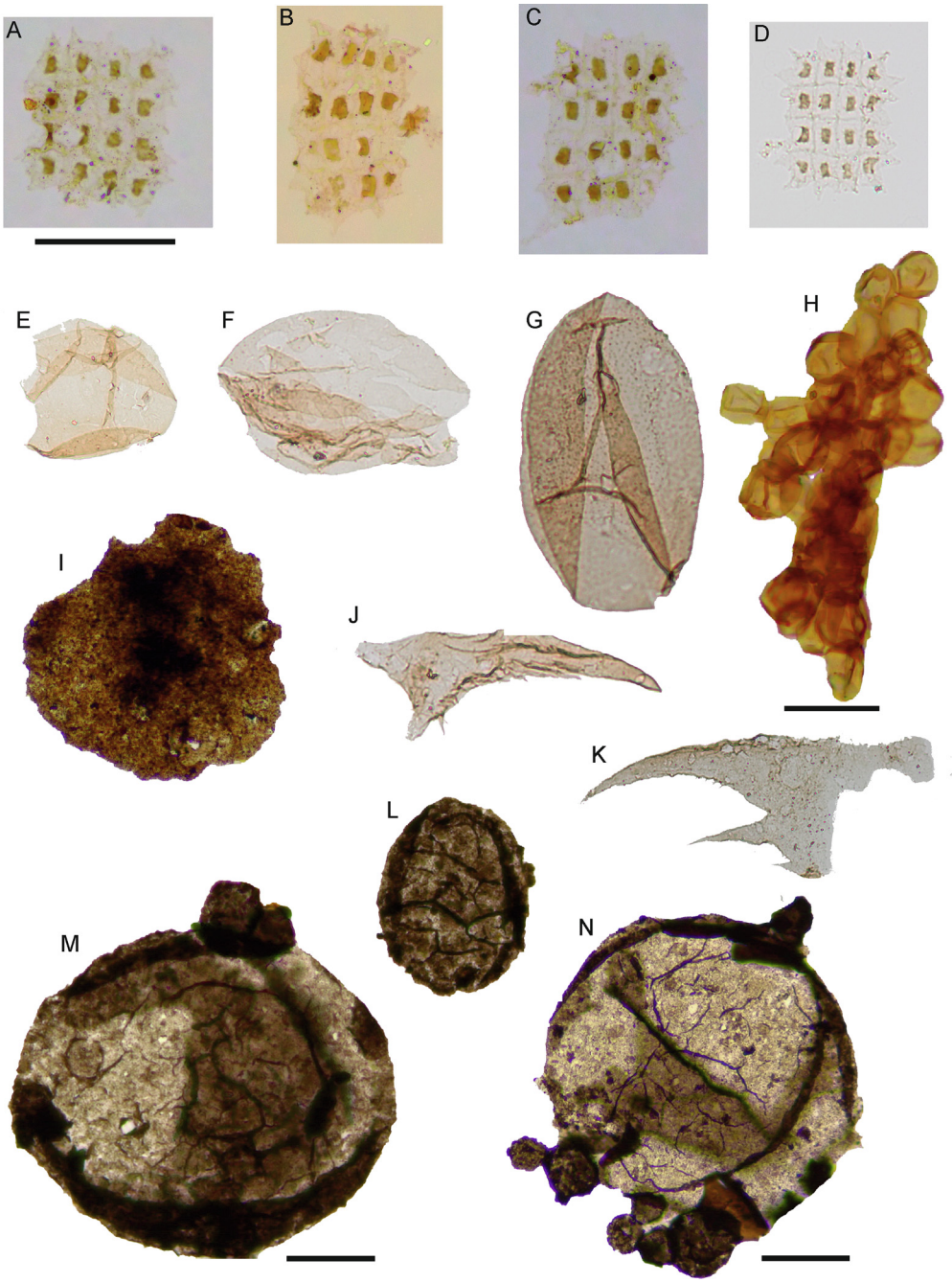

Fig. 6. Selected aquatic material from the Silves Group sections studied in this work. Species name is followed by the outcrop, sample, slide number and England Finder coordinates. **A.** *Plaesiodictyon mosellanum* ssp. *variable* Willie, 1970, outcrop Amado's Beach, sample AM15, slide 1Z, EF S38|4. **B.** *Plaesiodictyon mosellanum* ssp. *variable* Willie, 1970, outcrop Amado's Beach, sample AM15, slide 1, EF N47|3. **C.** *Plaesiodictyon mosellanum* ssp. *variable* Willie, 1970, outcrop Amado's Beach, sample AM15, slide 1Z, EF O37|3. **D.** *Plaesiodictyon mosellanum* ssp. *variable* Willie, 1970, outcrop Amado's Beach, sample AM15, slide 1Z, EF O34. **E.** *Leiosphaeridia* sp., outcrop Amado's Beach, sample AM15, slide 1Z, EF H17|4. **F.** *Ovoidites* sp., outcrop Amado's Beach, sample AM15, slide 1Z, EF P27. **G.** Algae sp. A, outcrop Amado's Beach, sample AM15, slide 1Z, EF K39|4. **H.** Fungal remains, outcrop Amado's Beach, sample AM15, slide 1Z, EF T38|2. **I.** *Botryococcus* sp., outcrop Amado's Beach, sample AM16, slide 1Z, EF K34. **J.**?Scolecodont or?insect, outcrop Amado's Beach, sample AM15, slide 1, EF M43. **K.**?Scolecodont or?insect, outcrop Amado's Beach, sample AM15, slide 1, EF E32. **L.**?*Ourasphaira giraldae*, outcrop Rock Salt Mine, sample MSG1, slide 1, EF R28|1. **M.**?*Ourasphaira giraldae*, outcrop Rock Salt Mine, sample MSG1, slide 1, EF P21. **N.**?*Ourasphaira giraldae*, outcrop Rock Salt Mine, sample MSG1, slide 1, EF L41|3. Scale bars: 50 μm. (For interpretation of the references to color in this figure legend, the reader is referred to the web version of this article.)

era and six species of pollen, six genera and four species of spores, and one genus of algae, ranging from moderate to well-preserved. The FA of *Cerebropollenites macroverrucosus*, *Cerebropollenites* sp., and *Perinopollenites elatoides* distinguishes this assemblage. Other components include the pollen *Alisporites diaphanus*, *Araucariacites australis*, *Araucariacites* sp, malformed specimens of *Classopollis* sp., *Classopollis meyerianus*, *Classopollis torosus*, *Classopollis* sp., *Cycadopites* sp., and *Ephedripites* sp. Additionally, the spores *Anapiculatisporites* sp., *Calamospora mesozoica*, *Calamospora* sp., *Deltoidospora toralis*, *Deltoidospora* sp., *Kraeuselisporites reissingeri*, *Kraeuselisporites* sp., *Kyrtomisporis* sp. and *Leptolepidites argentaeformis* are present. The algae *Leiosphaeridia* sp. is also identified.

The palynoassemblage recovered from the Albufeira's Diapir consists of two genera and two species of pollens, two genera of

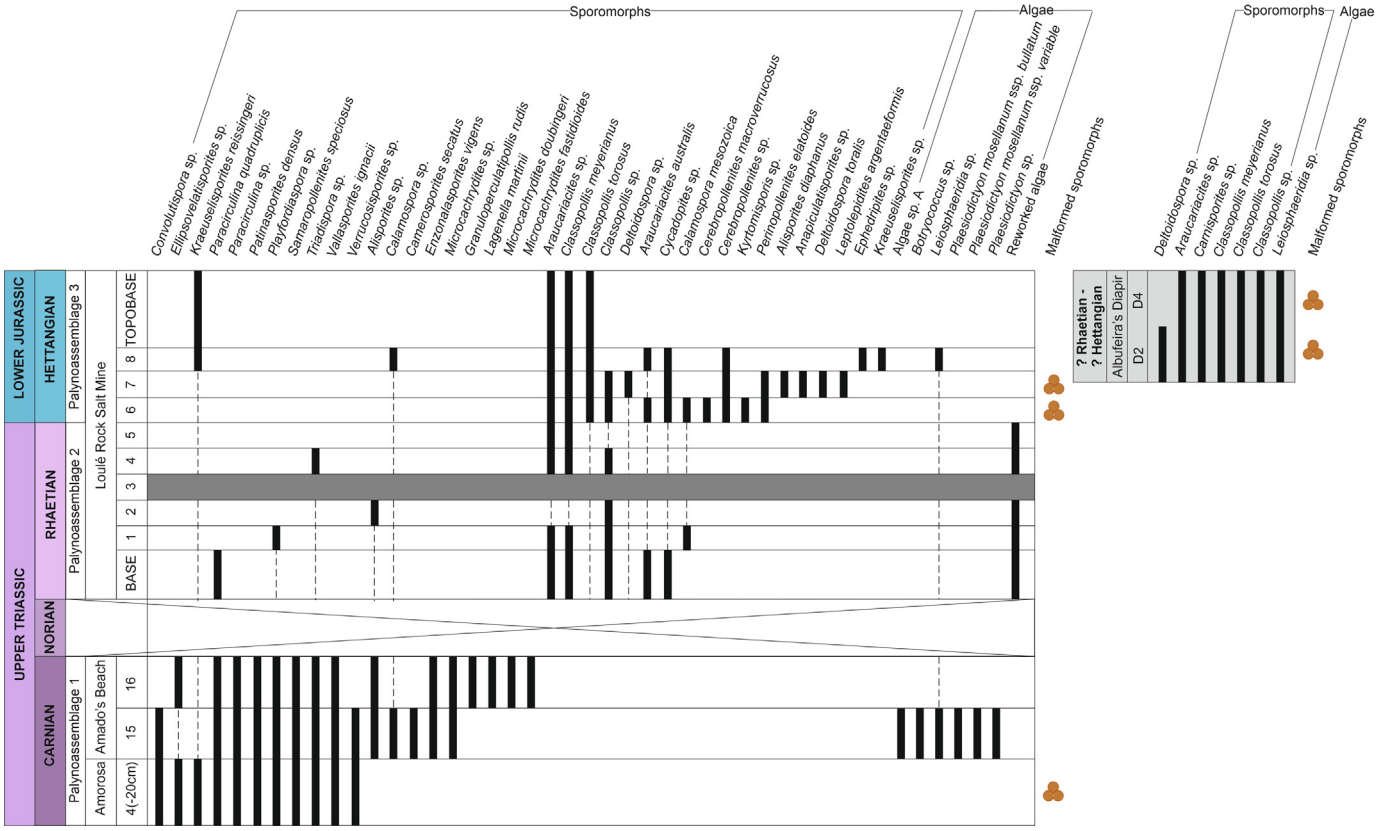

Fig. 7. Composite range chart of the sporomorphs and algae found in the Silves Group, Algarve Basin. Dark grey band represents barren palynological sample. Light grey band represents the Albufeira's Diapir section, whose stratigraphical position is not certain. The tetrad symbols on the right of the chart sign samples that have malformed sporomorphs in their palynological content. The data from Albufeira's Diapir is presented outside from the principal graphic because the succession does not provide age information. (For interpretation of the references to color in this figure legend, the reader is referred to the web version of this article.)

spores, and one genus of algae; the material is moderately well preserved. The assemblage includes the pollen *Araucariacites* sp., malformed specimens of *Classopollis* sp., *Classopollis meyerianus*, *Classopollis* sp., *Classopollis torosus* and *Cycadopites* sp., and the spores *Deltoidospora* sp. and *Carnisporites* sp. The algae *Leiosphaeridia* sp. is also present.

4. Discussion

4.1. Age of Silves Group

By correlating the present results with those from Vilas-Boas et al., (2022), we can reconstruct the entire stratigraphic succession of the Silves Group.

4.1.1. Lower part of Silves Sandstones

This part of the Silves Group has been dated as early Carnian based on a palynological assemblage found in a 3 m thick layer situated 2.5 m above the Variscan unconformity in the North of Portimão (Vilas-Boas et al., 2022). The assemblage includes *Alisporites* sp., *Aulisporites astigmosus*, *Cycadopites* sp., *Enzonalasporites vigens*, *Nevesisporites* cf. *vallatus*, *Ovalipollis pseudoalatus*,?*Protodiploxypinus* sp., *Samaropollenites speciosus*, *Triadispora* sp., *Tulesporites briscoensis* and *Vallasporites ignacii*, along with the spores *Calamospora* sp., *Conbaculatisporites* sp., *Converrucosisporites* sp., *Deltoidospora* sp.,?*Klausipollenites* sp., *Lycopodiacidites rugulatus* and *Verrucosisporites* sp. It is worth noting the presence of *A. astigmosus* which, along with *E. vigens*, *S. speciosus* and *T. briscoensis*, suggests a mixture of early Carnian palynofloral elements with affinities to Central European and North American domains, consistent with the paleogeographic position of the Iberian Peninsula at that time (Palain, 1976; Terrinha et al., 2013; Vilas-Boas et al., 2022).

4.1.2. Uppermost Silves Sandstones

This portion of the Silves Sandstones was sampled at the Amorosa section. The presence of a significant abundance of Circumpolles such as *Paracirculina quadruplicis*, along with the monosaccate pollen *Patinasporites densus* and the bisaccate pollen *Samaropollenites speciosus* indicates a palynological record of Carnian age (Mehdi et al., 2009; Cirilli, 2010; Buratti et al., 2012). Furthermore, the presence of *Ellipsovelatisporites* sp., *Triadispora* sp. and *Vallasporites ignacii*, in conjunction with the other palynological findings, enables the dating of the uppermost part of the Silves Sandstones to the upper Carnian (Schuurman, 1977, 1979; Visscher and Krystyn, 1978; Visscher et al., 1980; Visscher and Brugman, 1981; Van der Eem, 1983; Fisher and Dunay, 1984; Blendinger, 1988; Hochuli et al., 1989; Cirilli and Eshet, 1991; Cirilli and Montanari, 1994; Broglio Loriga et al., 1999; Hochuli and Frank, 2000; Warrington, 2002; Roghi, 2004; Mietto et al., 2007; Cirilli, 2010).

4.1.3. Lowermost part of the Silves Marl-Carbonate Evaporitic Complex

The basal portion of this unit was studied along the northern cliffs of Amado Beach, Aljezur. The significant presence of *Paracirculina quadruplicis*, *Paracirculina* sp., *Camerosporites secatus* and *Patinasporites densus*, along with *Ellipsovelatisporites* sp., *Enzonalasporites vigens* and *Triadispora* sp. indicates a Carnian age as documented in the European domain (phase 1 of Schuurman, 1977, 1979; Dolby and Balme, 1976; Buratti and Cirilli, 2007; Cirilli,

2010; Kürschner and Herngreen, 2010; Mietto et al., 2012). In Central and North-Western Europe, the Carnian-Norian boundary is marked by the LAD of *Camerosporites secatus* (Cirilli, 2010; Kürschner and Herngreen, 2010). Furthermore, the presence of *Granuloperculatipollis rudis*, which FO was dated as Tuvalian (Kürschner and Herngreen, 2010; Mietto et al., 2012; Kustatscher et al., 2018) and of *Lagenella martinii* which LO was referred to the same substage in the European domain (Kürschner and Herngreen, 2010), constrains the age of the lower part of the Silves Marl-Carbonate Evaporitic Complex to the upper Carnian.

4.1.4. Uppermost Silves Marl-Carbonate Evaporitic Complex

The evaporite rocks at the top of this sequence were sampled in the Loulé Rock Salt Mine. The palynological assemblage is dominated by *Araucariacites* sp., *Classopollis meyerianus* and *Classopollis torosus*; it is characterized by an increase in *Kraeuselisporites reissingeri*. The FO of *Cerebropollenites macroverrucosus, Cerebropollenites* sp. and *Perinopollenites elatoides* at the top of the sampled succession indicates a Hettangian age for top of this section. The absence of this taxa together with the absence of significant Carnian-early Norian forms such as *Camerosporites* spp., *Ellipsovelatisporites* spp., *Enzonalasporites* spp., *P. densus*, *Rhaetipollis germanicus* and *V. ignacii* along with *G. rudis* at the base of the section points to an upper Rhaetian age for the basal part (Morbey, 1975; Schuurman, 1977, 1979; Visscher et al., 1980; Fisher and Dunay, 1981; Visscher and Brugman, 1981; Cirilli, 2010). Therefore, this interval encompasses the Triassic/Jurassic boundary, as it occurs in other different sections in Europe (Clement-Westerhof et al., 1974; Morbey, 1975, 1978; Van Erve, 1977; Visscher et al., 1980; Fisher and Dunay, 1981; Kürschner et al., 2007; Kürschner and Herngreen, 2010). Based on palynological findings, an overall upper Rhaetian to lowermost Hettangian age is indicated for the uppermost part of the Silves Marl-Carbonate Evaporitic Complex represented in the Loulé Rock Salt Mine.

The palynoassemblage of the samples recovered from the Albufeira's Diapir is very poor and dominated by *Classopollis meyerianus*, *Classopollis torosus*, *Classopollis* sp., and malformed specimens of *Classopollis* sp. with common *Araucariacites* sp. The malformed specimens of *Classopollis* sp., when in tetrads, exhibit one of the four grains of the tetrad that appears much darker and smaller, sometimes with lack of ornamentation compared to the other pollen grains. These abnormalities in the aspect of the pollen grains of *Classopollis* sp. could be indicative of environmental stress related to atmospheric pollution, volcanic mercury (that could be related to the Eastern North America CAMP volcanism), and UVB radiation, generating mutagenesis in the land plants at the end of the Triassic (Visscher et al., 2004; Foster and Afonin, 2005; Whiteside et al., 2007, 2010; Cirilli et al., 2009; Filipiak and Racki, 2010; Kürschner et al., 2013; Hochuli et al., 2017; Lindström et al., 2019; Vajda et al., 2023). The lack of typical age-indicative sporomorphs does not allow us to determine this section's age more precisely and better define stratigraphic constraints. However, considering the similarity with the palynoassemblage from the Loulé Rock Salt Mine, both of which represent the evaporitic part of this unit, a possible Rhaetian-Hettangian age could be indicated for the Albufeira's Diapir.

Table 2
List of sporomorph and algal genera found in the Silves Group, Algarve Basin, and their probable botanical affinities and ecological remarks.

Genus	Botanical affinity	Ecological Remarks
Pollen		
Alisporites spp.	seed fern, Corystospermales, Peltaspermales	xerophytic, upper canopy, mire, wet lowland/hinterland, inhabit upland seasonally dry habitats
Araucariacites spp.	conifer, Araucariaceae	xerophytic, upper canopy, well drained, coastal
Camerosporites spp.	Cheirolepidiaceae	xerophytic, hinterland
Cerebropollenites spp.	conifer, Taxodiaceae	hygrophytic, upper canopy, well drained
Classopollis spp.	conifer, Cheirolepidiaceae	xerophytic, upper canopy, well drained, coastal, lowland, drier, warmer
Cycadopites spp.	gymnosperm, Cycadophyta, Ginkgoales, Peltaspermales	hygrophytic, dry lowland, warmer
Ellipsovelatisporites spp.	conifer	xerophytic, (?)hinterland/upland
Enzolasporites spp.	conifer, Voltziales, Majonicaceae, Glyptolepis	xerophytic, (?)hinterland/upland
Ephedripites spp.	gymnosperm, Gnetales, Ephredraceae	Unknown
Granuloperculatipollis spp.	conifer, Cheirolepidiaceae	upper canopy, well drained
Lagenella spp.	gymnosperm, Spermatophyta, Gentopsida, Gnetales	hygrophytic, river, lowland
Microcachrydites spp.	Podocarpaceae	xerophytic, upland, hinterland
Paracirculina spp.	Unknown	Unknown
Patinasporites spp.	conifer, Voltziales, Majonicaceae	xerophytic, (?)dryland, upland, dry lowland
Perinopollenites spp.	conifer, Cupressaceae/Taxodiaceae	hygrophytic, upper canopy, mire, river
Samaropollenites spp.	conifer	Unknown
Triadispora spp.	conifer, Voltziaceae	xerophytic, upland, hinterland
Vallasporites spp.	conifer, Voltziales, Majonicaceae	xerophytic, hinterland, dry lowland, upland
Spore		
Anapiculatisporites spp.	lycopsids, fern, moss?	hygrophytic, ground cover, mire, coastal, river/lowland, wet lowland
Calamospora spp.	horsetails, Sphenophyta, Equisetopsids	hygrophytic, river, lowland, wetter, warmer, acquire wet habitat in sub-tropical and temperate regions
Carnisporites spp.	lycophyta, Filicales	hygrophytic, river, wet lowland
Convolutispora sp.	Schizaeales	Unknown
Deltoidospora spp.	pteridophyta, fern, Filicales - Dicksoniaceae, Cyatheaceae, Dipteridaceae, Matoniaceae	hygrophytic, understory, mire, drier patches, dry lowland
Kraeuselisporites spp.	Lycopodiophyta; Lycopsida; Lycopodiales	hygrophytic, ground cover, mire, coastal, river
Kyrtomisporis spp.	pteridophyta, fern, Dipteridaceae	hygropghytic, river, (?)dry lowland
Leptolepidites spp.	Filicopsida; Filicales; Pteridaceae	(?)wet lowland
Playfordiaspora spp.	lycopsids	stress tolerant opportunistc plants which grow near water bodies
Verrucosisporites spp.	pteridophyta, Ferns, Marattiales, Filicales especially Osmundaceae	hygrophytic, river, wet lowland, acquire wet habitat in sub-tropical and temperate regions
Algae		
Botryococcus spp.	chlorococcale green algae, Dictyosphaeriaceae	open water, brackish/freshwater
Leiosphaeridia spp.	Prasinophyceae	marine, swamp, lake/pond
Ovoidites spp.	Zygnemataceae, Spirogyra	shallow, stagnant, oxygen-rich fresh waters, lake margins
Plaesiodictyon mosellanum spp.	chlorococcale green algae	brackish/freshwater

4.2. Palaeoclimatology and paleoenvironmental inferences

A correlation between palynomorphs and the ecological affinity of their parent plants has been attempted, to provide data for palaeoclimatological and palaeoenvironmental reconstructions. In Table 2, a list of selected Triassic–Jurassic spore-pollen genera, their probable parent plant affinities, and possible ecological and climatological preferences is given (Bonis and Kürschner, 2012; Césari and Colombi, 2016; Paterson et al., 2016; Lindström et al., 2017; Li et al., 2018; Mishra et al., 2018; Baranyi et al., 2019; Tverdokhlebov et al., 2020). Based on the water needs of the different plants and/or their adaptability to adapt to dry environments, the sporomorphs were divided into two groups, those related to hygrophytic environments, plants that preferentially thrive in wet environments, and those pertaining to xerophytic plants adapted for growth under dry conditions (Bonis and Kürschner, 2012; Césari and Colombi, 2016; Paterson et al., 2016; Lindström et al., 2017; Li et al., 2018; Mishra et al., 2018; Baranyi et al., 2019; Tverdokhlebov et al., 2020). The "Unknown Affinity" includes species for which there is not enough data available to assign them a botanical affinity.

Based on the quantitative analysis we recognize that the xerophytic plants are the most abundant in all sampled successions (Figs. 8, 9). At the top of the Silves Sandstones, most of the palynological content (ca. 75%) does not allow us to determine an environmental preference, due to the unknown botanical affinity or ecological characteristics of these plants (Figs. 8, 9). However, out of the ca. 25% of the palynological material for which we were able to associate an environmental preference, 16% consists of xerophytic plants (e.g., *Ellipsovelatisporites* sp., *Patinasporites densus*, *Triadispora* sp., and *Vallasporites ignacii*), while 8.6% consists of hygrophytic plants (e.g., *Convolutispora* sp., *Kraeuselisporites reissingeri*, *Leptolepidites argentaeformis*, and *Verrucosisporites* sp.). At the base of the Silves Marl-Carbonate Evaporitic Complex, there is an increase in xerophytic plants (e.g., *Alisporites* sp., *Camerosporites secatus*, *Ellipsovelatisporites* sp., *Enzonalasporites ignacii*, *Microcachrydites* spp., *Patinasporites densus*, *Triadispora* sp., and *Vallasporites ignacii*), accounting for up to 27.8%, and a decrease in hygrophytic plants (e.g., *Calamospora* sp., *Kraeuselisporites reissingeri*, *Lagenella martini*, and *Verrucosisporites* sp.), with a maximum of 2.6% (Figs. 8, 9). Approaching the top of the Silves Marl-Carbonate Evaporitic Complex, at the Triassic-Jurassic transition, there is a significant increase in xerophytic plants (*Alisporites* sp., *Araucariacites* sp., *Classopollis meyerianus*, *Classopollis* sp., and *Triadispora* sp.) ranging from 75% to 93%, along with almost no presence of hygrophytic type-plants (*Calamospora mesozoica* and *Playfordiaspora* sp.) at the top of the Rhaetian (Figs. 8, 9). At the base of the Hettangian, the palynological content is dominated by xerophytic plants (*Alisporites diaphanus*, *Araucariacites australis*, *Araucariacites* sp., *Classopollis meyerianus*, *Classopollis torosus*, and *Classopollis* sp.) accounting for 95% to 99% of the assemblage, with the hygrophytics plants (represented by the pollen and spore taxa *Cycadopites* sp., *Perinopollenites elatoides*, *Anapiculatisporites* sp., *Calamospora mesozoica*, *Deltoidospora toralis*, *Deltoidospora* sp., *Kraeuselisporites reissingeri*, and *Kyrtomisporis* sp.) consistently present but in very low percentages, ca. 2.5% (Figs. 8, 9). This increase in xerophytic plants towards the top of the section aligns with the sedimentary facies observed at the top of the Silves Group, which consists of sulphate evaporites deposited in a sabkha environment. This is primarily observed through the presence of conifer sporo-

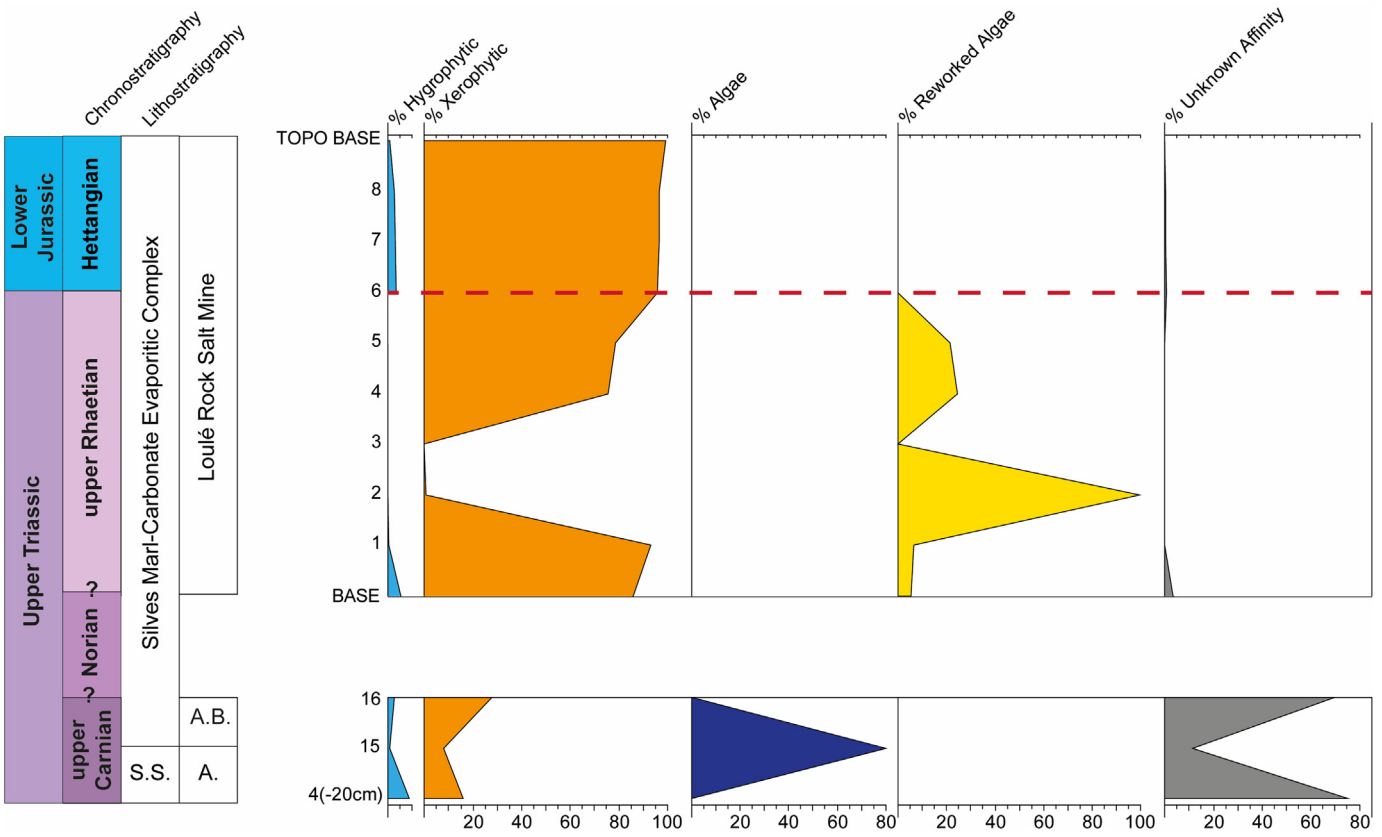

Fig. 8. Stratigraphic distribution of the palynological assemblages based on their probable botanical affinities. S.S.: Silves Sandstones; A.: Amorosa section; A.B.: Amado Beach section. (For interpretation of the references to color in this figure legend, the reader is referred to the web version of this article.)

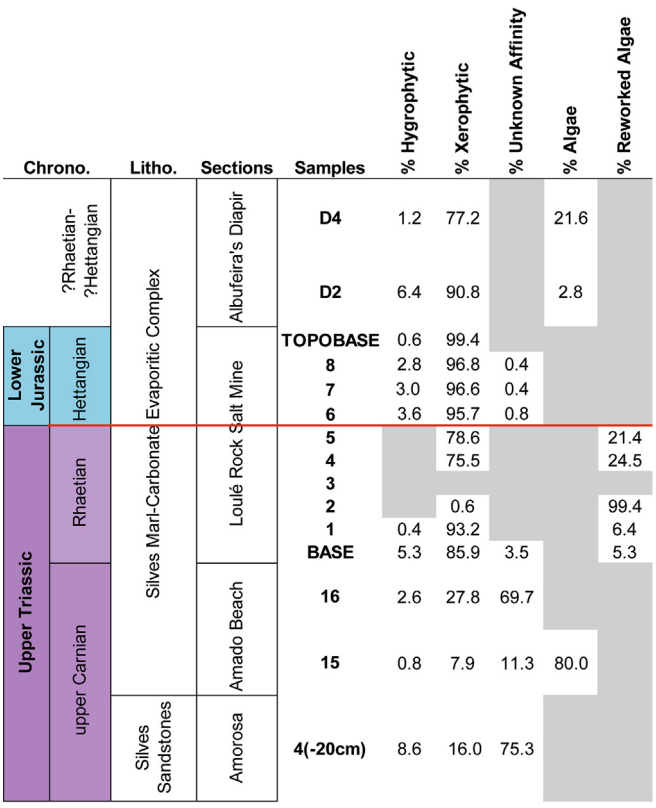

Fig. 9. Dataset (%) for the stratigraphical distribution of the palynological assemblage based on their probable botanical affinities. Light grey cells: no data; Chrono.: Chronostratigraphy; Litho.: Lithostratigraphy. (For interpretation of the references to color in this figure legend, the reader is referred to the web version of this article.)

morphs such as *Ellipsovelatisporites* sp., *Enzonalasporites vigens*, *Microcachrydites* spp., *Patinasporites densus*, *Triadispora* sp. and *Vallasporites ignacii*, and with the *Classopollis* group and *Araucariacites* sp. which become prominent upwards in the upper Rhaetian-Lower Jurassic strata.

The *Classopollis* group is produced by the Cheirolepidiaceae, one of the most prominent and diverse families of Mesozoic conifers. This extinct conifer family, believed to be related to the Cupressaceae or Araucariaceae, occupied a wide range of ecological niches and displayed diverse growth habits indicating warm conditions (Abbink, 1998; Buratti and Cirilli, 2007; Kürschner et al., 2013; Lindström, 2016). This data suggests a shift towards drier conditions during the Upper Triassic to Lower Jurassic, which aligns well with the lithofacies of this interval of the Silves Marl-Carbonate Evaporitic Complex, referred to as a coastal sabkha depositional setting. The presence of malformed sporomorphs in the upper Carnian and at the base of Hettangian may provide information about climate conditions in terms of atmospheric pollution, volcanic mercury (associated with CAMP volcanism), and/or UVB radiation (Visscher et al., 2004; Foster and Afonin, 2005; Whiteside et al., 2007, 2010; Cirilli et al., 2009; Filipiak and Racki, 2010; Kürschner et al., 2013; Hochuli et al., 2017; Lindström et al., 2019).

The algae have the lowest representation within the successions, making their first appearance at the base of the Silves Marl-Carbonate Evaporitic Complex, in the upper Carnian, constituting 80% of the palynological assemblage (*Botryococcus* sp., *Leiosphaeridia* sp., *Ovoidites* sp., *Plaesiodictyon mosellanum* ssp. *bullatum*, *Plaesiodictyon mosellanum* ssp. *variable*, *Plaesiodictyon* sp.; Figs. 8, 9).

At the top of the Silves Marl-Carbonate Evaporitic Complex, reworked algae possibly from the Neo-Proterozoic become prevalent in the assemblage, from 5% to a maximum of 99%; being the only algal material present at the top of this unit (Figs. 8, 9). Reworked material is palynological material eroded, transported, and redeposited into sediments of a stratigraphically different age. At the beginning of the Hettangian, the algae disappear, similar to the end of the Permian (Mays et al., 2020; Vajda et al., 2020). The presence and the rapid increase of freshwater/brackish algae like *Botryococcus* sp., *Leiosphaeridia* sp., *Ovoidites* sp., *Plaesiodictyon mosellanum* ssp. *bullatum* and *Plaesiodictyon mosellanum* ssp. *variable* at the base of the Silves Marl-Carbonate Evaporitic Complex indicates a seawater influence and the establishment of a coastal environment during the upper Carnian. This suggests that during the deposition of the Silves Marl-Carbonate Evaporitic Complex, there was a transition from a continental environment in the lower Carnian, represented by the underlying siliciclastic red beds of the Silves Sandstones, to a coastal-lacustrine environment in the upper Carnian. The presence of reworked Neo-Proterozoic algae (e.g., *Ourasphaira giraldae*) in the upper Rhaetian successions of the Silves Marl-Carbonate Evaporitic Complex, suggests a significant increase in the rate of erosion in the continental area, leading to the transportation of older material into the sedimentary environment. The absence of Norian to lower Rhaetian terranes in the studied area aligns with the hypothesis of a regional relative sea-level fall and a regressive episode, exposing extensive continental areas to erosion. It is worth noting that this interpretation is based in the colour and the degradation of that material; this is a working hypothesis that will require further confirmation through additional sedimentological and stratigraphic data.

4.3. Palaeophytogeographic implications

The microfloral assemblage documented in the study area, spanning from the upper Carnian to the Triassic/Jurassic boundary, provides new insights into understanding microfloristic provincialism and palaeophytogeographic implications during this important time interval. The palynological assemblage from the upper Carnian of the Silves Group includes taxa such as *Camerosporites secatus*, *Enzonalasporites vigens*, *Paracirculina quadruplicis*, *Paracirculina* sp., *Patinasporites densus*, *Samaropollenites speciosus* and *Vallasporites ignacii*, which are typical of the Onslow microflora. The occurrence of bisaccate pollen is rare; however, the presence of *Samaropollenites speciosus*, a crucial taxon for palaeofloristic reconstructions, along with other typical southern elements such as *Enzonalasporites vigens*, *Patinasporites densus* and *Vallasporites ignacii*, suggests an Onslow microflora affinity for several localities of the northern hemisphere (Visscher and Krystyn, 1978; Besems, 1982; Fisher and Dunay, 1984; Adloff et al., 1985; Cirilli and Eshet, 1991; Litwin et al., 1991; Cirilli and Montanari, 1994; Gòczàn and Oravecz-Scheffer, 1996; Broglio Loriga et al., 1999; Roghi, 2004; Buratti and Cirilli, 2007; Traverse, 2007; Cirilli, 2010). This microfloral province, comprising a mixture of Gondwana and European taxa, extended across western Europe and northwestern Australia, and it characterized continental margins under warm temperate climate, likely influenced by a monsoonal regime (Dolby and Balme, 1976; Cirilli and Eshet, 1991; Foster et al., 1994; Buratti and Cirilli, 2007; Cirilli, 2010; Césari and Colombi, 2013, 2016; Cirilli et al., 2015, 2018). In conjunction with that documented in the basal Silves Sandstones of the Silves Group (Vilas-Boas et al., 2022), it provides further evidence of the extension of the Onslow Microflora into the Western Tethys.

During the latest Triassic (Norian), the emergence and spread of the Cheirolepidiaceae (Circumpolles producers) represent another significant floral event, triggering a gradual decrease in Late Triassic microfloral provincialism and subsequently leading to the glo-

bal dispersal of a more homogenous Early Jurassic flora (Cirilli, 2010). The occurrence of the *Classopollis* (= Circumpolles) group, among other Gondwanan taxa, in the Upper Triassic-Lower Jurassic assemblages of Europe is attributed to the migration of the Cheirolepidiaceae plants from the southern areas of the Tethyan region to higher latitudes in the Late Triassic-Early Jurassic, during a warm climatic phase (Cirilli, 2010; Cirilli et al., 2015, 2018). It is likely that the Cheirolepidiaceae expanded through coastal migration routes formed by the Carnian-Norian plate rearrangement (Martini et al., 1997, 2004; Buratti and Cirilli, 2007; Cirilli, 2010). The presence of this group in the Algarve Basin and the Lusitanian Basin (Vilas-Boas et al., 2021, 2022) confirms its global distribution, indicating a gradual decline in microfloral provincialism leading into the Lower Jurassic. Also, the increase in Cheirolepidiaceae is accompanied with a decrease in plants with hygrophytic affinity.

5. Conclusions

The palynological study of the Silves Group in the Algarve Basin leads to the following conclusions.

For the first time, it is possible to assign an age to the entire stratigraphic succession of the Silves Group, from the lower Carnian to the lower Hettangian (Triassic/Jurassic boundary included) based on palynostratigraphy. Previous research had dated the base of Silves Sandstones as lower Carnian. In this study, the upper part of the Silves Sandstones is dated as upper Carnian. The basal part of the Silves Marl-Carbonate Evaporitic Complex is dated as upper Carnian, and the upper part of this unit is dated as upper Rhaetian-lower Hettangian. In the upper Carnian, at the base of the Silves Marl-Carbonate Evaporitic Complex, the appearance and rapid increase of algal spores (e.g., *Plaesiodictyon mosellanum* ssp. *variable*, *Plaesiodictyon mosellanum* ssp. *bullatum*, *Botryococcus* spp., and *Ovoidites* sp.), which adapted well to brackish water environments, support the lithological evidence of a transition from a continental fluvial setting (Silves Sandstones) to a coastal environment with swamps, ponds and lagoons (base of Silves Marl-Carbonate Evaporitic Complex).

The quantitative analysis of xerophytic vs. hygrophytic sporomorph categories, reveals a consistent increase of plants with xerophytic affinities upwards in the Silves Group, indicating a shift toward warmer and drier conditions from the upper Carnian to the lower Hettangian. This trend aligns with lithofacies evidence, which suggests an evolution from a coastal pond/lagoon environment (base of Silves Marl-Carbonate Evaporitic Complex) to a sabkha depositional setting (top of Silves Marl-Carbonate Evaporitic Complex). The presence of malformed sporomorphs in the upper Carnian and lower Hettangian may indicate environmental changes, potentially in response to external environmental stressors such as atmospheric pollution, volcanic mercury, and/or UVB radiation. The presence of *Ourasphaira giraldae* (reworked Neo-Proterozoic algae) at the top of the Silves Marl-Carbonate Complex (upper Rhaetian) suggests increased erosion during that time, leading to the transport and redeposition of older material. The absence of Norian and lower Rhaetian terranes in the studied area, supports the hypothesis of a brief regressive episode, that exposed those areas to erosion.

Finally, the lower Carnian to upper Carnian interval in the Silves Group exhibits a microflora that correlates with the Onslow Microflora, distributed along the continental margins of the southwestern Tethys. This correlation provides new insights into the microfloral distribution during this period and offers information about the climate in the Algarve Basin during Carnian. In the uppermost Triassic, another significant microfloral event is recorded, marked by the increased diffusion of the Cheirolepidiaceae into the Lower Jurassic. This event indicates the migration of the Circumpolles producers to higher latitudes within the context of plate rearrangement.

CRediT authorship contribution statement

Margarida Vilas-Boas: Conceptualization, Data curation, Formal analysis, Funding acquisition, Investigation, Methodology, Project administration, Resources, Software, Supervision, Validation, Visualization, Writing – original draft, Writing – review & editing. **Zélia Pereira:** Conceptualization, Data curation, Formal analysis, Funding acquisition, Methodology, Supervision, Validation, Visualization, Writing – review & editing. **Simonetta Cirilli:** Data curation, Formal analysis, Resources, Supervision, Validation, Visualization, Writing – review & editing. **Paulo Fernandes:** Conceptualization, Data curation, Formal analysis, Funding acquisition, Investigation, Methodology, Project administration, Resources, Supervision, Validation, Visualization, Writing – review & editing.

Data availability

Data will be made available on request.

Declaration of competing interest

The authors declare that they have no known competing financial interests or personal relationships that could have appeared to influence the work reported in this paper.

Acknowledgments

Margarida Vilas-Boas is a Ph.D. student at the University of Algarve, with a scholarship awarded by the Fundação para a Ciência e Tecnologia (FCT) with the reference SFRH/BD/144125/2019. This study had the support of national funds through FCT, under the project LA/P/0069/2020 granted to the Associate Laboratory ARNET and UID/00350/2020 CIMA. SC acknowledges MUR project PRIN 2017RX9XXXY and PRIN 2022APF9M2, the Research Funds 2021-2023 (University of Perugia), Action Line: Climate, Energy and Mobility - WP5.2, Climate changes: scientific models, technology, and social impacts and PRIN Project 2022 - cod 2022APF9M2 - ALVIN (P.I. S. Cirilli). LNEG's technician Irene Sousa is acknowledged for laboratory support and sample preparation. We thank Alexandre Andrade for his support and availability during the Loulé Rock Salt Mine visits.

Appendix A. List of palynomorphs taxa

List of all palynomorphs taxa which were recovered from the material of Silves Group in the Algarve Basin studied herein, with full author citations. The taxa are listed alphabetically in three groups: spores, pollen, and algae.

Spores

Anapiculatisporites sp.
Calamospora mesozoica Couper, 1958
Calamospora sp.
Carnisporites sp.
Convolutispora sp.
Deltoidospora sp.
Deltoidospora toralis (Leschick) Lund, 1977
Kraeuselisporites reissingeri (Harris, 1957) Morbey, 1975.
Kraeuselisporites sp.
Kyrtomisporis sp.
Leptolepidites argentaeformis (Bolkhovitina) Morbey, 1975.

Playfordiaspora sp.
Verrucosisporites sp.

Pollen

Alisporites diaphanus (Pautsch, 1958) Lund, 1977
Alisporites sp.
Araucariacites australis Cookson, 1947
Araucariacites sp.
Camerosporites secatus Leschik, 1956 emend. Scheuring, 1978
Cerebropollenites macroverrucosus (Thiergart, 1949) Schulz, 1967
Cerebropollenites sp.
Classopollis meyerianus (Klaus 1960) Venkatachala et Goczan, 1964
Classopollis sp.
Classopollis torosus Reissinger, 1950
Cycadopites sp.
Ellipsovelatisporites sp.
Enzonalasporites vigens Leschik, 1955 emend. Scheuring, 1970
Ephedripites sp.
Granuloperculatipollis rudis (Venkatachala et Góczán, 1964) Scheuring, 1978
Lagenella martinii (Leschik, 1955) Klaus, 1960
Microcachrydites doubingeri Klaus, 1964
Microcachrydites fastidioides (Jansonius) Klaus, 1964
Microcachrydites sp.
Paracirculina quadruplicis Scheuring, 1970
Paracirculina sp.
Patinasporites densus Leschik emend. Scheuring, 1970
Perinopollenites elatoides Couper, 1958
Samaropollenites speciosus Goubin, 1965
Triadispora sp.
Vallasporites ignacii Leschik, 1956 emend. Scheuring, 1970

Algae

Algae sp. A
Botryococcus sp.
Leiosphaeridia spp.
Ovoidites sp.
Plaesiodictyon mosellanum ssp. *bullatum* Willie, 1970
Plaesiodictyon mosellanum ssp. *variable* Willie, 1970
Plaesiodictyon sp.
?Ourasphaira giraldae

References

Abbink, O.A., 1998. Palynological investigations in the Jurassic of the North Sea region. In: LPP Contribution Series 8. LPP Foundation, University of Utrecht, p. 192 p..

Adloff, M.C., Doubinger, J., Massa, D., Vachard, D., 1985. Trias de Tripolitaine (Libye). Nouvelles données biostratigraphiques et palynologiques. Première partie. Revue de l'Institut Français du Pétrole 40, 723–753.

Baranyi, V., Rostási, Á., Raucsik, B., Kürschner, W.M., 2019. Palynological and X-ray fluorescence (XRF) data of Carnian (Late Triassic) formations from western Hungary. Data in brief 23, 103858.

Besems, R.E., 1982. Aspects of Middle and Late Triassic Palynology. 4. On the Triassic of the External Zone of the Betic Cordilleras in the Province of Jaén Southern Spain (with a note on the presence of Cretaceous palynomorphs in a presumed "Keuper"section). Proceedings of the Koninklijke Nederlandse Akademie, Wetenschappen 85, 1–27.

Blendinger, E., 1988. Palynostratigraphy of the late Ladinian and Carnian in the southeastern Dolomites. Review of Palaeobotany and Palynology 53, 329–348.

Bonis, N.R., Kürschner, W.M., 2012. Vegetation history, diversity patterns, and climate change across the Triassic/Jurassic boundary. Paleobiology 38, 240–264.

Broglio Loriga, C., Cirilli, S., De Zanche, V., Di Bari, D., Gianolla, P., Laghi, G.F., Lowrie, W., Manfrin, S., Mastandrea, A., Mietto, P., Muttoni, G., Neri, C., Posenato, R., Reichichi, M., Rettori, R., Roghi, G., 1999. The Prati di Stuores/Stuores Wiesen section (Dolomites, Italy): a candidate global stratotype section and point for the base of the Carnian stage. Rivista Italiana Paleontologia e Stratigrafia 105, 37–78.

Brusatte, S.L., Butler, R.J., Mateus, O., Steyer, J.S., 2015. A new species of Metoposaurus from the Late Triassic of Portugal and comments on the systematics and biogeography of metoposaurid temnospondyls. Journal Vertebrate Paleontology 35, e912988.

Buratti, N., Cirilli, S., 2007. Microfloristic provincialism in the Upper Triassic Circum-Mediterranean area and palaeogeographic implication. Geobios 40, 133–142.

Buratti, N., Mehdi, D., Cirilli, S., Kamoun, F., Mzoughi, M., 2012. A Carnian (Julian) microflora from the Djerba Melita 1 borehole (Gulf of Gabes, South-eastern Tunisia). Micropaleontology 58, 377–388.

César, S.N., Colombi, C.E., 2013. A new Late Triassic phytogeographical scenario in westernmost Gondwana. Nature Communications 4, 1889.

César, S.N., Colombi, C.E., 2016. Palynology of the Late Triassic Ischigualasto Formation, Argentina: paleoecological and paleogeographic implications. Palaeogeography, Palaeoclimatology, Palaeoecology 449, 365–384.

Cirilli, S., 2010. Upper Triassic–lowermost Jurassic palynology and palynostratigraphy: a review. Geological Society, London, Special Publications 334, 285–314.

Cirilli, S., Buratti, N., Gugliotti, L., Frixa, A., 2015. Palynostratigraphy and palynofacies of the Upper Triassic Streppenosa Formation (SE Sicily, Italy) and inference on the main controlling factors in the organic rich shale deposition. Review of Palaeobotany and Palynology 218, 67–79.

Cirilli, S., Eshet, Y., 1991. First discovery of Samaropollenites and the Onslow Microflora in the Upper Triassic of Israel, and its phytogeographic implications. Palaeogeography, Palaeoclimatology, Palaeoecology 85, 207–212.

Cirilli, S., Marzoli, A., Tanner, L., Bertrand, H., Buratti, N., Jourdan, F., Bellieni, G., Kontak, D., Renne, P.R., 2009. Latest Triassic onset of the Central Atlantic magmatic province (CAMP) volcanism in the Fundy basin (Nova Scotia): new stratigraphic constraints. Earth and Planetary Science Letters 286, 514–525.

Cirilli, S., Montanari, L., 1994. The Carnian evaporites succession of Bistriça River (southern Albany). Palaeopelagos 4, 107–118.

Cirilli, S., Panfili, G., Buratti, N., Frixa, A., 2018. Paleoenvironmental reconstruction by means of palynofacies and lithofacies analyses: an example from the Upper Triassic subsurface succession of the Hyblean Plateau Petroleum System (SE Sicily, Italy). Review of Palaeobotany and Palynology 253, 70–87.

Clement-Westerhof, J.A., Van Der Eem, J.G.L.A., Van Erve, A.W., Klasen, J.J., Schuurman, W.M.L., Visscher, H., 1974. Aspects of Permian, Triassic and Early Jurassic palynology of western Europe - a research project. Geologie en Mijnbouw 53, 329–341.

Dolby, J.H., Balme, B.E., 1976. Triassic palynology of the Carnarvon Basin, Western Australia. Review of Palaeobotany and Palynology 22, 105–168.

Filipiak, P., Racki, G., 2010. Proliferation of abnormal palynoflora during the end-Devonian biotic crisis. Geological Quarterly 54, 1–14.

Fisher, M.J., Dunay, R.E., 1981. Palynology and the Triassic/Jurassic boundary. Review of Palaeobotany and Palynology 34, 129–135.

Fisher, M.J., Dunay, R.E., 1984. Palynology of the petrified forest member of the Chinle Formation (Upper Triassic), Arizona, USA. Pollen et spores 26, 241–284.

Foster, C.B., Afonin, S.A., 2005. Abnormal pollen grains: an outcome of deteriorating atmospheric conditions around the Permian-Triassic boundary. Journal of the Geological Society, London 162, 653–659.

Foster, C.B., Balme, B.E., Helby, R., 1994. First record of Tethyan palynomorphs from the Late Triassic of East Antarctica. AGSO Journal of Australian Geology and Geophysics 15, 239–246.

Góczán, F., Oravecz-Scheffer, A., 1996. Tuvalian sequence of the Balaton Highland and the Zsámbék Basin: Part II. Characterization of sporomorph and foraminifer assemblages, biostratigraphic, palaeogeographic and geohistoric conclusion. Acta Geologica Hungarica 39, 33–101.

Hochuli, P.A., Colin, J.P., Vigran, J.O., 1989. Triassic biostratigraphy of the Barents Sea area. In: Correlation in Hydrocarbon Exploration. Proceedings of the conference Correlation in Hydrocarbon Exploration organized by the Norwegian Petroleum Society and held in Bergen, Norway, 3–5 October 1988, Dordrecht: Springer Netherlands, pp. 131–153.

Hochuli, P.A., Frank, S.M., 2000. Palynology (dinoflagellate cysts, spore-pollen) and stratigraphy of the Lower Carnian Raibl Group in the Eastern Swiss Alps. Eclogae Geologicae Helvetiae 93, 429–444.

Hochuli, P.A., Schneebeli-Hermann, E., Mangerud, G., Bucher, H., 2017. Evidence for atmospheric pollution across the Permian-Triassic transition. Geology 45, 1123–1126.

Kürschner, W.M., Batenburg, S.J., Mander, L., 2013. Aberrant *Classopollis* pollen reveals evidence for unreduced (2n) pollen in the conifer family Cheirolepidiaceae during the Triassic–Jurassic transition. Proceedings of the Royal Society B: Biological Sciences 280, 20131708.

Kürschner, W.M., Bonis, N.R., Krystyn, L., 2007. Carbon-isotope stratigraphy and palynostratigraphy of the Triassic-Jurassic transition in the Tiefengraben-section Northern Calcareous Alps (Austria). Palaeogeography, Palaeoclimatology, Palaeoecology 244, 257–280.

Kürschner, W.M., Herngreen, G.W., 2010. Triassic palynology of central and northwestern Europe: A review of palynofloral diversity patterns and biostratigraphic subdivisions. The Geological Society, London, Special Publications 334, 263–283.

Kustatscher, E., Ash, S. R., Karasev, E., Pott, C., Vajda, V., Yu, J., McLoughlin, S., 2018. Flora of the late Triassic. In: The Late Triassic World: Earth in a Time of Transition, pp. 545–622.

Li, L., Wang, Y., Vajda, V., Liu, Z., 2018. Late Triassic ecosystem variations inferred by palynological records from Hechuan, southern Sichuan Basin, China. Geological Magazine 155, 1793–1810.

Lindström, S., 2016. Palynofloral patterns of terrestrial ecosystem change during the end-Triassic event–a review. Geological Magazine 153, 223–251.

Lindström, S., Erlström, M., Piasecki, S., Nielsen, L.H., Mathiesen, A., 2017. Palynology and terrestrial ecosystem change of the Middle Triassic to lowermost Jurassic succession of the eastern Danish Basin. Review of Palaeobotany and Palynology 244, 65–95.
Lindström, S., Sanei, H., Van De Schootbrugge, B., Pedersen, G.K., Lesher, C.E., Tegner, C., Heunisch, C., Dybkjær, K., Outridge, P.M., 2019. Volcanic mercury and mutagenesis in land plants during the end-Triassic mass extinction. Science Advances 5, eaaw4018.
Litwin, R.J., Traverse, A., Ash, S.R., 1991. Preliminary palynological zonation of the Chinle Formation, southwestern USA, and its correlation to the Newark Supergroup (eastern USA). Review of Palaeobotany and Palynology 68, 269–287.
Martini, R., Vachard, D., Zaninetti, L., Cirilli, S., Cornée, J.J., Lathuilière, B., Villeneuve, M., 1997. Sedimentology, stratigraphy and micropaleontology of the Upper Triassic reefal series in Eastern Sulawesi (Indonesia). Palaeogeography, Palaeoclimatology, Palaeoecology 128, 157–174.
Martini, R., Zaninetti, L., Lathuillière, B., Cirilli, S., Cornée, J.J., Villeneuve, M., 2004. Upper Triassic carbonate deposits of Seram (Indonesia): palaeogeographic and geodynamic implications. Palaeogeography, Palaeoclimatology, Palaeoecology 206, 75–102.
Mateus, O., Butler, R.J., Brusatte, S.L., Whiteside, J.H., Steyer, J.S., 2014. The first phytosaur (Diapsida, Archosauriformes) from the Late Triassic of the Iberian Peninsula. Journal of Vertebrate Paleontology 34, 970–975.
Mays, C., Vajda, V., Frank, T.D., Fielding, C.R., Nicoll, R.S., Tevyaw, A.P., McLoughlin, S., 2020. Refined Permian-Triassic floristic timeline reveals early collapse and delayed recovery of south polar terrestrial ecosystems. GSA Bulletin 132, 1489–1513.
Mehdi, D., Cirilli, S., Buratti, N., Kamoun, F., Trigui, A., 2009. Palynological characterisation of the Lower Carnian of the Kea5 borehole (Koudiat El Halfa Dome; Central Atlas, Tunisia). Geobios 42, 63–71.
Mietto, P., Andreetta, R., Broglio Loriga, C., Buratti, N., Cirilli, S., De Zanche, V., Furin, S., Gianolla, P., Manfrin, S., Muttoni, G., Neri, C., Nicora, A., Posenato, R., Preto, N., Rigo, M., Roghi, G., Spötl, C., 2007. A candidate of the Global Boundary Stratotype Section and Point for the base of the Carnian Stage (Upper Triassic): GSSP at the base of the canadensis Subzone (FAD of Daxatina) in the Prati di Stuores/Stuores Wiesen section (Southern Alps, NE Italy). Albertiana 36, 78–97.
Mietto, P., Manfrin, S., Preto, N., Rigo, M., Roghi, G., Furin, S., Gianolla, P., Posenato, R., Muttoni, G., Nicora, A., Buratti, N., Cirilli, S., Spötl, C., Ramezani, J., Bowring, S. A., 2012. The global boundary stratotype section and point (GSSP) of the Carnian stage (Late Triassic) at Prati di Stuores/Stuores Wiesen section (Southern Alps, NE Italy). Episodes 35, 414.
Mishra, S., Aggarwal, N., Jha, N., 2018. Palaeoenvironmental change across the Permian-Triassic boundary inferred from palynomorph assemblages (Godavari Graben, south India). Palaeobiodiversity and Palaeoenvironments 98, 177–204.
Morbey, S.J., 1975. The palynostratigraphy of the Rhaetian stage, Upper Triassic in the Kendelbachgraben, Austria. Palaeontographica B 152, 1–75.
Morbey, S.J., 1978. Late Triassic and Early Jurassic subsurface palynostratigraphy in northwestern Europe. Palinologia 1 (spec. issue), 355–368.
Palain, C., 1976. Une série détritique terrigène les "Grès de Silves": Trias et Lias inférieur du Portugal. Memória dos Serviços Geológicos de Portugal 25, 377 p.
Paterson, N.W., Mangerud, G., Mørk, A., 2016. Late Triassic (early Carnian) palynology of shallow stratigraphical core 7830/5-U-1, offshore Kong Karls Land, Norwegian Arctic. Palynology 41, 230–254.
Reolid, M., Muñiz Guinea, F., Toscano, A., Belaústegui, Z., 2022. First record of fossil sauropterygians from the Upper Triassic of Southwestern Spain (Ayamonte, Huelva province). Estudios Geológicos 78, e145.
Riding, J.B., Warny, S. (Eds.), 2008. Palynological Techniques. second ed. American Association of Stratigraphic Palynologists Foundation, Dallas, Texas, p. 137.
Roghi, G., 2004. Palynological investigations in the Carnian of the Cave del Predil area (Julian Alps, NE Italy). Review of Palaeobotany and Palynology 132, 1–35.
Santos, A., Popovic, N., Mayoral, E., 2022. Palaeoecology of Late Triassic marine assemblages from the proto-Atlantic Basin (Ayamonte, SW Spain). Proceedings of the Geologists' Association 133, 47–66.
Schuurman, W.M., 1977. Aspects of Late Triassic palynology. 2. Palynology of the "Grès et schiste à *Avicula contorta*" and "Argiles de levallois" (Rhaetian) of northeastern France and Southern Luxemburg. Review of Palaeobotany and Palynology 23, 159–253.
Schuurman, W.M., 1979. Aspects of Late Triassic palynology. 3. Palynology of latest Triassic and earliest Jurassic deposits of the northern Limestone Alps in Austria and southern Germany, with special reference to a palynological characterization of the Rhaetian Stage in Europe. Review of Palaeobotany and Palynology 27, 53–75.
Terrinha, P., Rocha, R.B., Rey, J., Cachão, M., Moura, D., Roque, C., Martins, L., Valadares, V., Cabral, J., Azevedo, M.R., Barbero, L., Clavijo, E., Dias, R.P., Matias, H., Madeira, J., Silva, C.M., Munhá, J., Rebelo, L., Ribeiro, C., Noiva, J., Youbi, N., Bensalah, M.K., 2013. A Bacia do Algarve: Estratigrafia, paleogeografia e tectónica. Geologia De Portugal, Geologia Meso-Cenozóica De Portugal II, 29–166.
Terrinha, P., Rocha, R.B., Rey, J., Cachão, M., Moura, D., Roque, C., Martins, L., Valadares, V., Cabral, J., Azevedo, M.R., Barbero, L., Clavijo, E., Dias, R.P., Matias, H., Madeira, J., Silva, C.M., Munhá, J., Rebelo, L., Ribeiro, C., Vicente, J., Noiva, J., Youbi, N., Bensalah, M.K., 2006. A Bacia do Algarve: Estratigrafia, paleogeografia e tectónica. Geologia de Portugal no contexto da Ibéria, 1–138.
Traverse, A., 2007. Paleopalynology, second ed. In: Landman, N.H., Jones, D.S. (Eds.), Topics in Geobiology Series, American Association of Stratigraphic Palynologists Foundation, Springer, Dordrecht 28, 814 p.
Tverdokhlebov, V.P., Sennikov, A.G., Novikov, I.V., Ilyina, N.V., 2020. The youngest Triassic land vertebrate assemblage of Russia: composition and dating. Paleontolological Journal 54, 297–310.
Vajda, V., McLoughlin, S., Mays, C., Frank, T.D., Fielding, C.R., Tevyaw, A., Lehsten, V., Bocking, M., Nicoll, R.S., 2020. End-Permian (252 Mya) deforestation, wildfires and flooding—An ancient biotic crisis with lessons for the present. Earth and Planetary Science Letters 529, 115875.
Vajda, V., McLoughlin, S., Slater, S.M., Gustafsson, O., Rasmusson, A.G., 2023. The 'seed-fern' *Lepidopteris* mass-produced the abnormal pollen *Ricciisporites* during the end-Triassic biotic crisis. Palaeogeography, Palaeoclimatology, Palaeoecology 627, 111723.
Van Der Eem, J.G.L.A., 1983. Aspects of middle and late Triassic palynology. 6. Palynological investigations in the Ladinian and lower Karnian of the Western Dolomites Italy. Review of Palaeobotany and Palynology 39, 189–300.
Van Erve, A.W., 1977. Palynological investigation in the lower Jurassic of the Vicentinian Apls (Northeastern Italy). Review of Palaeobotany and Palynology 23, 1–117.
Verati, C., Rapaille, C., Féraud, G., Marzoli, A., Bertrand, H., Youbi, N., 2007. $^{40}Ar/^{39}Ar$ ages and duration of the Central Atlantic Magmatic Province volcanism in Morocco and Portugal and its relation to the Triassic-Jurassic boundary. Palaeogeography, Palaeoclimatology, Palaeoecology 244, 308–325.
Vilas-Boas, M., Paterson, N.W., Pereira, Z., Fernandes, P., Cirilli, S., 2022. The age of the first pulse of continental rifting associated with the breakup of Pangea in Southwest Iberia: new palynological evidence. Journal of Iberian Geology 48, 181–190.
Vilas-Boas, M., Pereira, Z., Cirilli, S., Duarte, L.V., Fernandes, P., 2021. New data on the palynology of the Triassic-Jurassic boundary of the Silves Group, Lusitanian Basin, Portugal. Review of Palaeobotany and Palynology 290, 104426.
Visscher, H., Brugman, W.A., 1981. Ranges of selected palynomorphs in the Alpine Triassic of Europe. Review of Palaeobotonay and Palynology 34, 115–128.
Visscher, H., Krystyn, L., 1978. Aspects of Late Triassic palynology. 4. A palynological assemblage from ammonoid-controlled Late Karnian (Tuvalian) sediments of Sicily. Review of Palaeobotany and Palynology 26, 93–112.
Visscher, H., Looy, C.V., Collinson, M.E., Brinkhuis, H., van Konijnenburg-van Cittert, J.H.A., Kürschner, W.M., Sephton, M.A., 2004. Environmental mutagenesis during the end-Permian ecological crisis. Proceedings of the National Academy of Sciences 101, 12952–12956.
Visscher, H., Schuurman, W.M.L., Van Erve, A.W., 1980. Aspects of a palynological characterization of Late Triassic and Early Jurassic 'Standard' units of chronostratigraphical classification in Europe. Proceedings of the International Palynological Conference IV, Lucknow 2, 281–287.
Warrington, G., 2002. Triassic spores and pollen. In: Jansonius, J., Mcgregor, D.C. (Eds.), Palynology: Principles and Applications. American Association of Stratigraphic Palynologists Foundation, 2nd edition, pp. 755–766.
Whiteside, J.H., Olsen, P.E., Eglinton, T., Brookfield, M.E., Sambrotto, R.N., 2010. Compound-specific carbon isotopes from earth's largest flood basalt eruptions directly linked to the end-Triassic mass extinction. Proceedings of the National Academy of Sciences 107, 6721–6725.
Whiteside, J.H., Olsen, P.E., Kent, D.V., Fowell, S.J., Et-Touhami, M., 2007. Synchrony between the Central Atlantic magmatic province and the Triassic-Jurassic mass extinction event? Palaeogeography, Palaeoclimatology, Palaeoecology 244, 345–367.
Wood, G.D., Gabriel, A.M., Lawson, J.E., 1996. Palynological techniques - processing and microscopy. In: Jansonius, J., McGregor, D.C. (Eds.), Palynology: Principles and Applications. American Association of Stratigraphic Palynologists Foundation, Dallase 1, pp. 29–50.